A methodology to determine the seismic low-cycle fatigue strength of timber connections

Authors

Daniele Casagrande[1*], Stefano Bezzi[2], Giuseppe D'Arenzo[3,4], Sascha Schwendner[4], Andrea Polastri[1], Werner Seim[4], Maurizio Piazza[2]

Abstract

In this paper the seismic low-cyclic fatigue strength for different typologies of dissipative timber connections is analysed by means of a novel methodology, which defines an interaction between the strength degradation and the ductility capacity. The results of more than 40 cyclic tests on panel-to-timber, timber-to-timber, steel-to-timber connections and mechanical anchors are reported and discussed, by defining an approximated linear relationship between the slip amplitude and the impairment of strength from the 1st to 3rd cycle. A proposal for considering the strength degradation as an additional condition in the determination of ultimate slip of dissipative connections subjected to low-cyclic load testing is presented. The seismic low-cycle fatigue strength in terms of ductility capacity and strength degradation is compared for all the tested connection. Four different categories of connections in terms of low-cycle fatigue strength are proposed.

Keywords: seismic design; impairment of strength; strength degradation; dissipative connection; cyclic tests.

---

[1] Institute for BioEconomy - National Research Council of Italy (CNR-IBE), Italy;

[2] Department of Civil, Environmental and Mechanical Engineering, University of Trento, Italy;

[3] Faculty of Engineering and Architecture, Kore University of Enna, Italy;

[4] Building Rehabilitation and Timber Engineering, University of Kassel, Germany;

* **Corresponding author**; casagrande@ivalsa.cnr.it

1. Introduction

In recent years, timber structural systems have been increasingly becoming a viable alternative to other structural materials in seismic prone areas. Several research studies have shown a significant seismic capacity of timber structures mainly due to a high strength-to-weight ratio of engineered wood products (EWD) combined with a significant energy dissipation and displacement capacity related to the non-linear behaviour of mechanical connections. Experimental tests on full-scale structures and advanced numerical analyses have been carried out to investigate the seismic behaviour of traditional light-frame timber structures [12], [44], [47] and more recent structural systems such as Cross-Laminated Timber [4], [37], [39], [49], giving a strong input for the revision process and the improvement of Standard documents related to the seismic design of timber structures [16].

Due to the brittle nature of wood material, the dissipation of seismic energy together with deformation capacity in timber structures is typically achieved in mechanical connections through the yielding in bending of metal (steel) dowel-type fasteners, whereas the timber members themselves are regarded as behaving elastically. As a result, mechanical connections have to be designed in order to show adequate low-cyclic fatigue strength, developing plastic deformations with medium-to-high amplitude when subjected to cyclic loads.

The ability of connections to undergo plastic deformations, commonly defined as ductility, represents a fundamental requirement in seismic design of structures. Ductility is, in fact, strictly related to connection's energy dissipation capacity and ensures that connections satisfy the displacement or rotation local demand for high seismic events [26], [36].

The ductility capacity μ of timber connections is usually calculated, on a conventional basis, as the ratio between the ultimate v_u and yield slip amplitude v_y, see eq. 1, which are determined by means of quasi-static low-cyclic tests carried out through a displacement controlled loading procedure that involves deformation cycles grouped in phases (where the same value of deformation is achieved) at incrementally increasing slip levels, see Figure 1.

$$\mu = \frac{v_u}{v_y} \tag{1}$$

Although the concept of ductility appears straightforward in the field of the seismic behaviour of timber connections, there has been difficulty in reaching consensus within the scientific community as to a unique cyclic testing procedure and the appropriate definition of yield slip. Definitions and determination methods of seismic parameters from test data differ between each Standard document, with a consequent considerable variation in the estimation of ductility capacity of connections and assemblages [33].

The capacity to limit the degradation of the strength in a low-cycle test is the ability of structural elements to maintain a constant level of load under repetition of medium-to-high amplitude plastic deformations. In European Standard for cyclic testing of joints in timber structures [9], this capacity is usually determined by measuring the impairment ΔF in the load between the Envelope Load-Slip Curves (ELSCs), see Figure 1, related to the 1st and 3rd cycle when attaining a given slip amplitude v. A different approach is used in steel structures where the strength degradation of beam-to-column joints, [3], subjected to low-cyclic load testing, is defined as the loss of strength with reference to a nominal plastic capacity of the joint, calculated using codified calculation rules, independently on the number of cycles, at a certain value of slip amplitude. A similar procedure is proposed in the revision process of the European Standard [50] for the determination of the seismic ductility classes of dowel-type fasteners in timber structures. The fastener residual bending moment corresponding to a bending angle equal to 45°, after that the fastener had been previously subjected to three fully-reversed bending cycles, has to be higher than the 80% of the nominal yielding moment capacity [25].

The low-cyclic fatigue strength represents a key-parameter for the seismic behaviour of timber connections. High ductility associated with low strength degradation ensures a large amount of energy dissipation without a significant loss of strength.

Despite the importance of limiting the impairment of strength in timber connections subjected to medium-to-high amplitude cyclic loads, the strength degradation is not commonly taken into account in the determination of the connection’s ultimate slip. The condition to determine the ultimate slip is in fact usually related either by failure, a certain loss of the maximum load along the 1st cycle Envelope Load-Slip Loops Curves (1st ELSC) in the slip-softening branch or a certain maximum displacement. Strength degradation and ductility are hence considered as separate mechanical parameters in the analysis process of experimental results.

In this paper, the low-cyclic fatigue strength of different typologies of dissipative timber connections is analysed by means of a novel methodology, which defines an interaction between the strength degradation and the ductility capacity, offering two major contributions to the field:

i) it defines a relationship between the slip amplitude and the impairment of strength from the 1st to 3rd cycle;
ii) it considers the strength degradation as an additional condition for the determination of ultimate slip of dissipative connections subjected to low-cyclic load testing.

The results of 44 cyclic on panel-to-timber, timber-to-timber, steel-to-timber connections and mechanical anchors are evaluated and discussed. The study has been carried out within an international collaboration between Italian National Research Council of Italy, University of Trento (Italy) and University of Kassel (Germany). The discussion and the outcomes presented in this paper may represent a scientific support and background throughout the revision process of “timber” section of the Eurocode 8 [11] and the European Standard for cyclic testing of joints made with mechanical fasteners, EN 12512 [9].

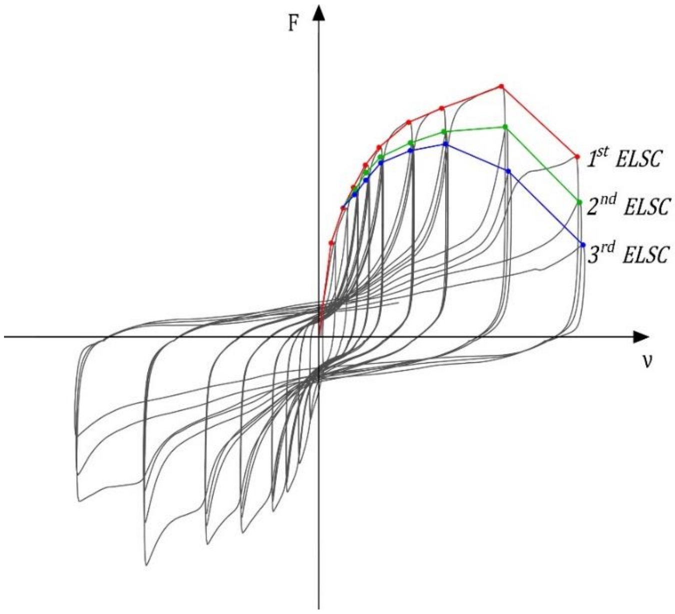

Figure 1: Envelope Load-Slip Curves (ELSCs) in quasi-static cyclic hysteresis loops of dowel-type fastener connections

2. Background

2.1 Cyclic testing on timber connections

The hysteretic behaviour of dissipative connections has been the focus of several research projects. Ductility, energy dissipation as well as strength degradation have been investigated for different types of timber-, panel- and steel-to-timber connections. A short summary of the state-of-the-art regarding the cyclic experimental tests on timber connections adopted as dissipative elements in Light-Frame Timber (LFT) and Cross-Laminated Timber (CLT) structures is reported hereafter.

The cyclic behaviour of LFT structures has largely explored in North America in last 50 years: Peterson [35] and Van de Lindt [46] gave a comprehensive overview in this field. With the aim to study the seismic performance of LFT structures, several tests were conducted by using different protocols for quasi-static cyclic testing on wood-framed walls. Stewart [43], Dolan and Madsen [8], Dean [7] have emphasized the importance of investigating the cyclic response of sheathing-to-framing nailed connections. Within the CUREE-Caltech project in USA, Fonseca et al. [17] carried out several tests to establish a large database for sheathing-to-wood connections which parameters necessary for modelling purposes can be extracted from. The cyclic behaviour of steel plate-to-foundation anchorage connections was investigated by Mahaney et al. [32]. Additional cyclic tests were performed on Oriented Strand Board (OSB)- and Plywood-to-solid wood nailed connections by Fischer et al. [13], according to the Curee-Caltech cyclic loading protocol developed by Krawinkler et al. [29]. The effects of cyclic loading protocols on the structural performance of LFT shear walls with OSB panels have been shown in He et al. [21]. Karakebeyli and Ceccotti [27] presented the results of quasi-static reversed cyclic tests on nailed joints for wood framed structures with different load testing protocols.

In Japan, Yasamura and Kawai [48] presented the result of cyclic tests on OSB, Gypsum and Plywood Sheathing-to-Framing connections whereas Kobayashi and Yasumura [28] evaluated cyclic response of plywood sheathed shear walls with screwed joints. More recently, in Italy, the ductility and strength degradation on OSB and Gypsum Fibre Boards (GFB) sheathing-to-framing connections under cyclic tests were investigated by Sartori and Tomasi [40], whereas Germano et al. [20] reported the results related to cyclic tests on Particle Board sheathing-to-framing connections. Within the OptimberQuake and OptimberquakeCheck projects, in Germany, Seim et al. [42] carried out a comparative study of cyclic behaviour of OSB vs GFB sheathing-to-framing connections and metal anchoring on CLT in terms of ductility, energy dissipation and load bearing capacity.

A large overview on testing connections to determine the seismic performance of CLT buildings is reported in Pei et al. [34] and Izzi et al. [24]. Gavric et al. [18] presented the results in terms of ductility and impairment of strength of hold-down and angle bracket connectors subjected to cyclic load tests within the SOFIE project. Similar results were presented by Flatscher et al. [14], in a test campaign within the SERIES project, and by Tomasi and Smith [45]. A deep investigation on the seismic performance of connections between CLT shear-wall panels and the foundation was also presented by Schneider et al. [41]. More recently, the axial-shear interaction on CLT hold-downs and angle brackets were investigated by Pozza et al. [38], D'Arenzo et al. [6] and Liu and Lam [30,31].

Concerning with the panel-to-panel connections, Gavric et al. [19] showed the good results in terms of ductility and energy dissipation on half-lapped and splice joints with partially threaded screws. Hossain et al. [22] conducted similar tests on panel-to-panel joints with double-angled fully threaded screws showing a higher stiffness and higher strength than those obtained with partially threaded screws.

Despite the large amount of experimental tests carried out on several different typologies of timber connections, the proposal of considering a relationship between the strength degradation and ductility in the determination of low-cycle fatigue strength has not been presented yet. No specific provision or limitation regarding the impairment of strength have been proposed in previous works. For this reason, as reported in the next section, in addition to the fact a not-unique interpretation can be given to demand in terms of low-cycle fatigue strength of timber connections in the current version of Eurocode 8, this paper presents a new proposal for the calculation of the low-cycle fatigue capacity.

2.2 Determination of mechanical properties from cyclic testing

Different methods for the determination of mechanical parameters (i.e. strength capacity, stiffness, ductility, etc.) from cyclic testing data are proposed in relevant Standard Documents. Several studies have highlighted the importance of achieving a general consensus within the research community to define a unique cyclic-test procedure and the appropriate definition of yield and ultimate slips in order to avoid inconsistencies due to such a high variability in the definition of the ductility.

He et al. [21] investigated the influence of cyclic testing protocols on performance of wood-based shear walls, showing the effects of cyclic load protocols on the structural performance of LFT shear walls built with nonstandard large dimension OSB panels. A comprehensive comparison between the different definitions of ductility has been presented by Munoz et al. [33] where are analysed and discussed the methods reported in: *i)* Karacabely and Ceccotti [27], *ii)* the European Standard EN12512 [9], *iii)* Commonwealth Scientific and Industrial Research Organisation [5], *iv)* Yasamura and Kawai [48], *v)* the National Design Specification for wood construction [1] and *vi)* the equivalent energy elastic-plastic (EEEP) approach proposed by Foliente [15].

2.2.1 Ultimate and yield slip according to EN12512, Kobayashi and Yasumura and ASTM E2126

Despite this paper does not aim to compare different approaches in the determination of the mechanical parameters from cyclic test data, the methods reported in the EN12512 [9], Kobayashi and Yasumura – K&Y [28] and the ASTM E2126 [2] are adopted to determine the strength degradation and ductility capacity of tested connections.

A good agreement between these three procedures has been achieved by the definition of the ultimate slip v_u. The ultimate condition is in fact determined by the slip corresponding to the failure of the specimen, by a load equal to the 80% of the maximum load after the achievement of the maximum load. In the definition of the yield slip v_y, conversely, three different methods are proposed.

In EN 12512 [9] the yield slip v_y can be calculated according to two different procedures. When the 1st ELSC presents two well defined linear parts, the yield slip v_y is determined by the intersection between the two lines (Method A). When two well defined linear parts are not observed, v_y is determined by the intersection of two additional lines (Method B): the first line (denoted as elastic line), with slope *K* (stiffness), is determined as that drawn through the point on curve corresponding to 10% of the maximum load F_{max} and the point on the curve corresponding to 40% of F_{max}. The second line (denoted as plastic line) is the tangent to the backbone curve having an inclination of 1/6 of the first line, see Figure 2. The ductility μ is calculated as the ratio between the ultimate v_u and the yield v_y slip, according to eq. 1.

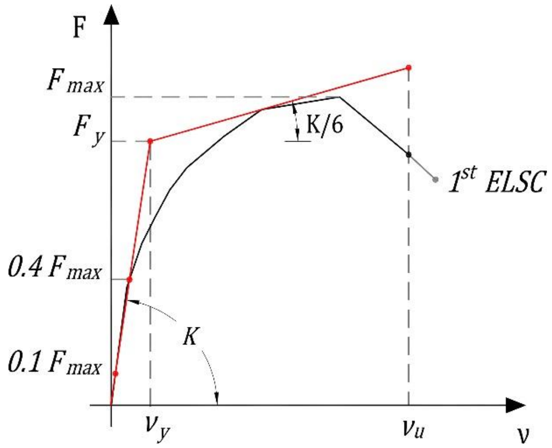

Figure 2: Determination of yield point (Method b) and ductility according to EN 12512 [9]

ASTM E2126 [2] and K&Y [28] apply the Equivalent Energy Elastic-Plastic (EEEP) method to determine the yield slip v_y and the ductility μ. The EEEP curve is determined by equating the area (A) under the 1st ELSC up to the ultimate slip v_u and the area limited by the two straight lines: the inclined line representing the EEEP stiffness and the horizontal line representing the EEEP load F_{EEEP}. The ductility is then calculated as the ratio between the ultimate slip v_u and the yield slip v_y, which is obtained by the intersection between the inclined and the horizontal EEEP lines.

In ASTM E2126 [2], the EEEP inclined line is obtained by connecting the origin to the point on the 1st ELSC corresponding to the 40% of the maximum load F_{max}, see Figure 3.

In K&Y [28] , the inclined line of the EEEP curve passes through the origin and a point on the backbone curve at the slip value v_y^* corresponding to the load P_y^* determined by the intersection of two other additional straight lines. The first of the two lines connects the points between 10% and 40% of the maximum load F_{max} whereas the second line is determined as the tangent to the backbone curve and parallel to the line connecting two points corresponding to 40% and 90% of the maximum load F_{max}, see Figure 4.

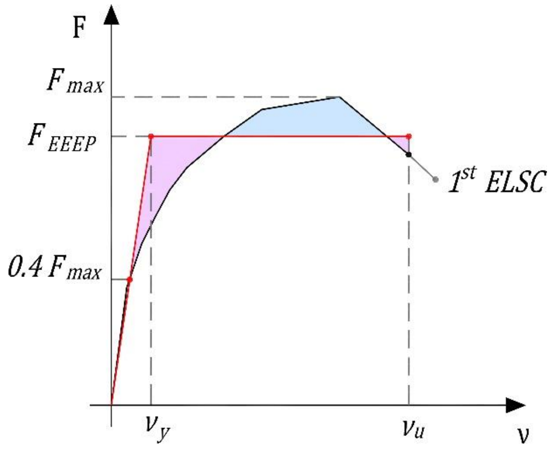

Figure 3: Determination of yield point and ductility according to ASTM E2126 [2]

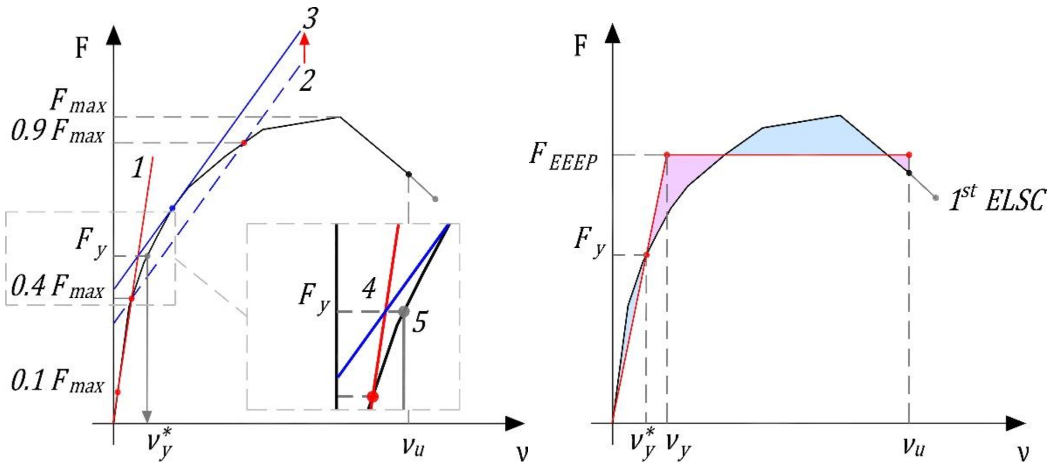

Figure 4: Determination of yield point and ductility according to K&Y [28]

2.3 Demand in terms of ductility capacity and strength degradation for dissipative connections according to Eurocode 8

The seismic demand in terms of low-cycle fatigue strength for dissipative connections in the current version of Eurocode 8 [11] is reported as: "*the dissipative zones shall be able to deform plastically for at least three fully reversed cycles at a static ductility ratio of 4 for ductility class Medium (DCM) structures and at a static ductility ratio of 6 for ductility class High structures (DCH), without more than a 20% reduction of their resistance".* According to that provision, the dissipative connections need to be designed to develop plastic deformations with a ductility capacity equal either to 4 or 6 depending on structure ductility class. Two different interpretations, however, can be given to the request related to the 20% "*reduction* *of their resistance*". It is not clear, in fact, if the reduction of resistance is referred to either the loss of strength along the softening branch of the 1st ELSC curve or to the impairment of strength between the 1st and the 3rd cycle at a value of slip corresponding to the requested ductility capacity. The former interpretation would be consistent with the procedure used for determination of the ultimate slip, corresponding to a value of load equal to the 80% of the peak load; however, in this case the impairment of strength ΔF between the 1st and 3rd cycle would not be taken into account. The latter interpretation would be consistent with the "short" loading procedure of EN12152 [9] where only three cycles at the same value of slip (corresponding to a pre-determined ductility) are performed to calculate the impairment of strength ΔF. However, no direct reference to the seismic demand in terms of low-cycle fatigue strength of Eurocode 8 is reported in EN12512.

In authors' opinion, the "short procedure" of EN12512 seems to reflect the provision of Eurocode 8 and therefore the "*reduction of resistance*" could be interpreted as the impairment of strength between the 1st and 3rd cycle. The same interpretation was assumed by Germano et al. [20] in the analyses of results from cycle-load tests on sheathing-to-framing connections: a limit equal to 20% for the impairment of strength ΔF between the 1st and 3rd cycle at values of ductility equal to either 4 or 6 was considered to verify the capacity of connections according to Eurocode 8. Nevertheless, it should be stated that impairment of strength is a somehow European phenomenon and a result of cycling testing according to European loading protocols with three successive loading steps for each slip level. In North America, where the focus had shifted from loading capacity to deformation capacity, testing of bracing elements under cyclic loading is carried out according to the CUREE protocol [29]. The CUREE protocol defines slightly reduced subsequent deformations on each level of the loading sequence, consequently impairment of strength disappears.

Since a not-unique interpretation to the provision reported in the current version of Eurocode 8 can be assumed, this paper proposes a new methodology for the determination of the low-cycle fatigue strength of dissipative connections, where ductility capacity, impairment of strength between the 1st and the 3rd cycle and the loss of strength related to a nominal value are taken into account simultaneously. The prospect of considering the strength degradation as an additional condition for the determination of ultimate displacements in low-cycle tests on connections is evaluated. For this purpose were analysed the results from three extended experimental campaigns, carried out at University of Trento (Italy) and University of Kassel (Germany) within the research projects X-Rev, OptimberQuake and OptimberquakeCheck, respectively. Additional tests were carried out specifically for this study at the Institute for BioEconomy - IBE (former IVALSA) of the National Research Council of Italy (CNR).

3. Materials and Methods

3.1 Materials and test layout

The cyclic load tests were performed on four different categories of connections, commonly considered as dissipative components in timber structures, namely panel-to-timber (P2T) connections, timber-to-timber (T2T) connections, steel-to-timber (S2T) connections and mechanical anchors (MA), i.e. hold-down and angle brackets.

Different typologies of fasteners, ring nails (RN), smooth nails (SN), staples (ST), annular-ringed shank nails (AN), self-tapping screws (SC) and dowels (DO) were investigated. For each category of connection, the test layout as well as the geometrical and mechanical properties of fasteners and wood-based members (solid wood - SW, glulam timber - GLT, cross-laminated timber - CLT), panels (oriented strand board panels – OSB, gypsum fibre board - GFB) and steel plates are reported in Tables 1-to-4. Due to the high variability of results in panel-to-timber connections, some of the results from Sartori and Tomasi [40] were also analysed and discussed.

For P2T connections, see Table 1, the same set-up was adopted in test at laboratories of

University of Trento (TN) and Kassel (KS), by connecting a solid wood element to two lateral panels. Each fastener was characterized by a single shear panel. The same test layout was used in the tests reported in [40].

Two different test layouts were adopted for the experimental tests on T2T connections. Single-shear plane glulam-to-glulam and double-shear plane CLT-to-CLT screwed connections were tested at laboratory of University of Trento (TN) and at the Institute for Bio-economy of the National Research Council of Italy (CNR), respectively. A double-shear plane CLT-to-CLT dowelled connection was tested at CNR laboratory as well, see Table 2.

For the test layout of S2T connection two GLT members were connected to a steel plate by means of either Anker nails (AN) or screws (SC). Each fastener was characterized by a single shear panel as shown in Table 3.

The tests on hold-downs were characterized by three different layouts. At TN and KS laboratories, a non-symmetric single hold-down test layout was adopted whereas for the test at CNR laboratory a symmetric double hold-down layout was chosen, see Table 4. At KS laboratory, an OSB and GFB panel was interlayered between the hold-down and the solid-wood member in the tests HD_OSB_1 and HD_GFB_01 respectively. The tests on angle brackets were carried out by connecting two CLT panels in AB_2 and AB_2, while in AB_1 the angle bracket was used to connect a steel beam to a CLT panel.

Table 1: Materials and test layout for panel-to-timber (P2T) connections

Test	Fasteners	Panel (P)	Timber member (T)	Lab.	Set-up
RN_OSB_1	RN - 2.8 x 80 mm -n: 7 - *sp*: 50 mm	OSB - *t*:15 mm - ρ=572 kg/m^3	SW - *t*: 160 mm- α:0° - in: 90°- ρ=439 kg/m^3	TN	
RN_OSB_2	RN - 2.8 x 60 mm -n: 7 - *sp*: 50 mm	OSB - *t*:15 mm - ρ=572 kg/m^3	SW - *t*: 160 mm- α:0° - in: 90°- ρ=439 kg/m^3	Sartori and Tomasi [40]	
RN_OSB_3	RN - 2.8 x 60 mm -n: 4 - *sp*: 100 mm	OSB - *t*:18 mm – ρ=581 kg/m^3	SW - *t*: 160 mm- α:0° - in: 90°- ρ=439 kg/m^3	Sartori and Tomasi [40]	
RN_OSB_4	RN - 2.8 x 60 mm- n: 7 - *sp*: 50 mm	OSB - *t*:18 mm - ρ=581 kg/m^3	SW - *t*: 160 mm- α:0° - in: 90°- ρ=439 kg/m^3	Sartori and Tomasi [40]	
SN_OSB_1	SN – 2.8 x 65 mm - n: 2 x 6 – *sp*: 40 mm	OSB - *t*:18 mm - ρ=581 kg/m^3	SW - *t*: 110 mm- α:0° - in: 90°- ρ=413 kg/m^3	KS	
SN_OSB_2	SN – 3.1 x 65 mm - n: 2 x 4 – *sp*: 80 mm	OSB - *t*:18 mm - ρ=581 kg/m^3	SW - *t*: 110 mm- α:0° - in: 90°- ρ=413 kg/m^3	KS	
SN_OSB_3	SN – 2.8 x 65 mm - n: 2 x 6 – *sp*: 40 mm	OSB - *t*:10 mm - ρ=583 kg/m^3	SW - *t*: 110 mm- α:0° - in: 90°- ρ=413 kg/m^3	KS	
SN_GFB_1	SN – 2.8 x 65 mm - n: 2 x 2 – *sp*: 80 mm	GFB - *t*:18 mm - ρ=1150 kg/m^3	SW - *t*: 110 mm- α:0° - in: 90°- ρ=413 kg/m^3	KS	
ST_OSB_1	ST – 1.53 x 55 mm - n: 2 x 6 – *sp*: 40 mm	OSB - *t*:10 mm - ρ=583 kg/m^3	SW - *t*: 110 mm- α:0° - in: 90°- ρ=413 kg/m^3	KS	
ST_OSB_2	ST – 1.53 x 35 mm - n: 2 x 6 – *sp*: 40 mm	OSB - *t*:18 mm - ρ=581 kg/m^3	SW - *t*: 110 mm- α:0° - in: 90°- ρ=413 kg/m^3	KS	
ST_OSB_3	ST – 1.8 x 55 mm - n: 2 x 6 – *sp*: 40 mm	OSB - *t*:18 mm - ρ=581 kg/m^3	SW - *t*: 110 mm- α:0° - in: 90°- ρ=413 kg/m^3	KS	
ST_GFB_1	ST – 1.53 x 55 mm - n: 2 x 2 – *sp*: 80 mm	GFB - *t*:18 mm - ρ=1150 kg/m^3	SW - *t*: 110 mm- α:0° - in: 90°- ρ=413 kg/m^3	KS	
ST_GFB_2	ST – 1.53 x 55 mm - n: 2 x 2 – *sp*: 80 mm	GFB - *t*:10 mm - ρ=1150 kg/m^3	SW - *t*: 110 mm- α:0° - in: 90°- ρ=413 kg/m^3	KS	
ST_GFB_3	ST–1.4x1.6x 55 mm – n: 4 – *sp*: 100 mm	GFB - *t*:12.5 mm - ρ=1150 kg/m^3	SW - *t*: 160 mm- α:0° - in: 90°- ρ=439 kg/m^3	Sartori and Tomasi [40]	

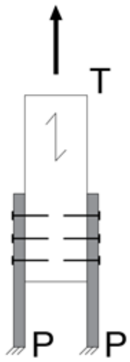

t: thickness of panels and timber member; ***sp***: spacing of fasteners; ***α***: angle between the load direction and timber member's grain direction; ***in****:* angle between the fastener and timber member's grain direction; ***ρ***: density of the timber member.

Table 2: Materials and test layout for timber-to-timber (T2T) connections

Test	Fasteners	Timber member A (T.A)	Timber member B (T.B)	Lab.	Set-up
SC_GLT_1	SC - 6 x 160 mm - n.5 - *sp*: 90 mm	GLT- *t*: 80 mm- α:0° - in: 90°- ρ=419 kg/m^3	GLT - *t*: 100 mm- α:0° - in: 90°- ρ=419 kg/m^3	TN	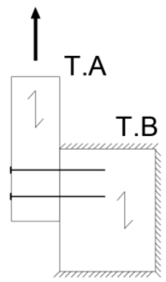
SC_GLT_2	SC - 6 x 160 mm - n.5 - *sp*: 90 mm	GLT- *t*: 80 mm- α:0° - in: 90°- ρ=419 kg/m^3	GLT - *t*: 100 mm- α:0° - in: 90°- ρ=419 kg/m^3	TN	
SC_GLT_3	SC - 8 x 160 mm - n.3 - *sp*: 140 mm	GLT - *t*: 80 mm- α:0° - in: 90°- ρ=419 kg/m^3	GLT - *t*: 100 mm- α:0° - in: 90°- ρ=419 kg/m^3	TN	
SC_GLT_4	SC - 8 x 160 mm - n.3 - *sp*: 140 mm	GLT - *t*: 80 mm- α:0° - in: 90°- ρ=419 kg/m^3	GLT - *t*: 100 mm- α:0° - in: 90°- ρ=419 kg/m^3	TN	
SC_GLT_5	SC - 10 x 160 mm - n.3 - *sp*: 140 mm	GLT - *t*: 80 mm- α:0° - in: 90°- ρ=419 kg/m^3	GLT - *t*: 100 mm- α:0° - in: 90°- ρ=419 kg/m^3	TN	
SC_GLT_6	SC - 10 x 160 mm - n.3 - *sp*: 140 mm	GLT - *t*: 80 mm- α:0° - in: 90°- ρ=419 kg/m^3	GLT - *t*: 100 mm- α:0° - in: 90°- ρ=419 kg/m^3	TN	
SC_CLT_1	SC - 6 x 300 mm - n.5 - *sp*: 160 mm	CLT - *t*: 100 mm- α:0° - in: 90°- ρ=420 kg/m^3	CLT - *t*: 100 mm- α:0° - in: 90°- ρ=420 kg/m^3	CNR	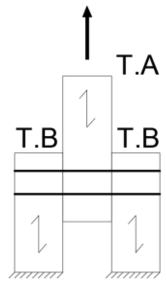
SC_CLT_2	SC - 8 x 300 mm - n.5 - *sp*: 160 mm	CLT - *t*: 100 mm- α:0° - in: 90°- ρ=420 kg/m^3	CLT - *t*: 100 mm- α:0° - in: 90°- ρ=420 kg/m^3	CNR	
SC_CLT_3	SC - 10 x 300 mm - n.5 - *sp*: 160 mm	CLT - *t*: 100 mm- α:0° - in: 90°- ρ=420 kg/m^3	CLT - *t*: 100 mm- α:0° - in: 90°- ρ=420 kg/m^3	CNR	
D_CLT_1	DO - 12 x 280 mm - n.5 - *sp*: 160 mm	CLT - *t*: 100 mm- α:0° - in: 90°- ρ=420 kg/m^3	CLT - *t*: 100 mm- α:0° - in: 90°- ρ=420 kg/m^3	CNR	

t: thickness of timber members; ***sp***: spacing of fasteners; ***α***: angle between the load direction and timber member's grain direction; ***in***: angle between the fastener and timber member's grain direction; ***ρ***: density of the timber member.

Table 3: Materials and test layout for steel-to-timber (S2T) connections

Test	Fasteners	Steel plate (S)	Timber member (T)	Protocol	Set-up
AN_S_1	AN - 4 x 60 mm -n: 8 - *sp*: 50 mm	S275 - *t*:3 mm - *b*: 80 mm	GLT - *t*: 100 mm- α:0° - in: 90°- ρ=419 kg/m^3	TN	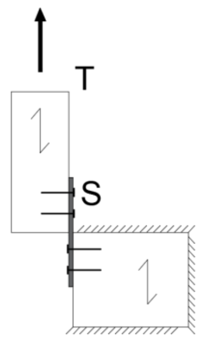
AN_S_2	AN - 4 x 60 mm -n: 8 - *sp*: 50 mm	S275 - *t*:3 mm - *b*: 80 mm	GLT - *t*: 100 mm- α:0° - in: 90°- ρ=419 kg/m^3	TN	
AN_S_3	AN - 4 x 60 mm -n: 8 - *sp*: 50 mm	S275 - *t*:6 mm - *b*: 80 mm	GLT - *t*: 100 mm- α:0° - in: 90°- ρ=419 kg/m^3	TN	
SC_S_1	SC - 5 x 60 mm -n: 8 - *sp*: 50 mm	S275 - *t*:3 mm - *b*: 80 mm	GLT - *t*: 100 mm- α:0° - in: 90°- ρ=419 kg/m^3	TN	
SC_S_2	SC - 5 x 60 mm -n: 8 - *sp*: 50 mm	S275 - *t*:3 mm - *b*: 80 mm	GLT - *t*: 100 mm- α:0° - in: 90°- ρ=419 kg/m^3	TN	
SC_S_3	SC - 5 x 60 mm -n: 8 - *sp*: 50 mm	S275 - *t*:6 mm - *b*: 80 mm	GLT - *t*: 100 mm- α:0° - in: 90°- ρ=419 kg/m^3	TN	

b: width of the steel plate; ***t***: thickness of steel plate and timber member; ***sp***: spacing of fasteners; ***α***: angle between the load direction and timber member's grain direction; ***in***: angle between the fastener and timber member's grain direction; ***ρ***: density of the timber member.

Table 4: Materials and test layout for mechanical anchors (MA)

Test	Fasteners	Mechanical anchor (M.A.)	Timber member (T) and Panel (P)	Lab.	Set-up
HD_SC_1	SC – 5x80 mm – n: 10 – *sp*: 20 mm	Hold-down S350 - *t*: 3 mm 559x62x64 mm	CLT - *t*: 120 mm- α:0° - in: 90°- *ρ*=426 kg/m^3	KS	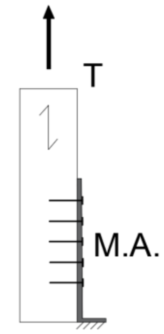
HD_AN_1	AN - 4x60 mm – n: 19 – *sp*: 20 mm	Hold-down S350 - *t*: 3 mm 559x62x64 mm	CLT - *t*: 120 mm- α:0° - in: 90°- *ρ*=426 kg/m^3	KS	
HD_AN_2	AN - 4 x 60 mm - n: 20 - *sp*: 20 mm	Hold-down – S275 - *t*: 3 mm - 340x60x63 mm	GLT - *t*: 100 mm- α:0° - in: 90°- *ρ*=419 kg/m^3	TN	
HD_AN_3	AN - 4 x 60 mm - n: 20 - *sp*: 20 mm	Hold-down - S275 - *t*: 3 mm - 340x60x63 mm	GLT - *t*: 100 mm- α:0° - in: 90°- *ρ*=419 kg/m^3	TN	
HD_AN_4	AN - 4 x 60 mm - n: 52 - *sp*: 20 mm	Hold-down – S275 - *t*: 3 mm - 620x60x63 mm	GLT - *t*: 100 mm- α:0° - in: 90°- *ρ*=419 kg/m^3	TN	
HD_AN_5	AN - 4 x 60 mm - n: 30 - *sp*: 20 mm	Hold-down – S275 - *t*: 3 mm - 620x60x63 mm	GLT - *t*: 100 mm- α:0° - in: 90°- *ρ*=419 kg/m^3	TN	
HD_AN_6	AN - 4 x 60 mm - n: 30 - *sp*: 20 mm	2 Hold-down - S275 - *t*: 3 mm - 440x60x63 mm	CLT - *t*: 100 mm- α:0° - in: 90°- *ρ*=420 kg/m^3	CNR	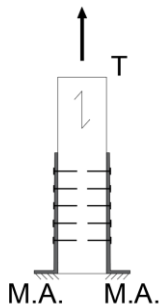
HD_AN_7	AN - 4 x 60 mm - n: 20 - *sp*: 20 mm	2 Hold-down - S275 - *t*: 3 mm - 440x60x63 mm	CLT - *t*: 100 mm- α:0° - in: 90°- *ρ*=420 kg/m^3	CNR	
HD_AN_8	AN - 4 x 60 mm - n: 45 - *sp*: 20 mm	2 Hold-down - S275 - *t*: 3 mm - 540x60x63 mm	CLT - *t*: 100 mm- α:0° - in: 90°- *ρ*=420 kg/m^3	CNR	
HD_OSB_1	AN - 4 x 60 mm - n: 17 - *sp*: 20 mm	Hold-down S235 - *t*: 2.8 mm 559x61x70 mm	SW - *t*: 120 mm- α:0° - in: 90°- *ρ*=413 kg/m^3 OSB - *t*:18 mm *ρ*=581 kg/m^3	KS	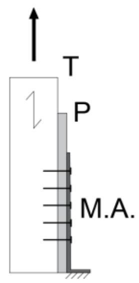
HD_GFB_1	AN - 4 x 60 mm - n: 17 - *sp*: 20 mm	Hold-down S235 - *t*: 2.8 mm 559x61x70 mm	SW - *t*: 120 mm- α:0° - in: 90°- *ρ*=413 kg/m^3 GFB - *t*:18 mm *ρ*=1150 kg/m^3	KS	
AB_1	AN - 4 x 60 mm - n: 30 - *sp*: 20 mm	Angle Bracket – S275 - *t*: 3 mm - 200x103x71mm	1 CLT panel - *t*: 100 mm- α:0°/90° - in: 90°- *ρ*=476 kg/m^3 / 1 steel beam	TN	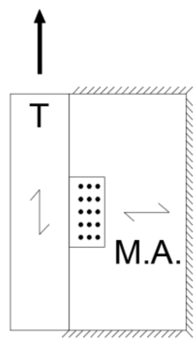
AB_2	AN - 4 x 60 mm - n: 30+30 - *sp*: 20 mm	Angle Bracket - S275 - *t*: 3 mm - 200x71x71mm	2 CLT panels - *t*: 100 mm- α:0°/90° - in: 90°- *ρ*=476 kg/m^3	TN	
AB_3	AN - 4 x 60 mm - n: 30+30 - *sp*: 20 mm	Angle Bracket - S275 - *t*: 3 mm - 200x71x71mm	2 CLT panels - *t*: 100 mm- α:0°/90° ° - in: 90°- *ρ*=476 kg/m^3	TN	

t: thickness of panels and timber member; ***sp***: spacing of fasteners; ***α***: angle between the load direction and timber member's grain direction; ***in:*** angle between the fastener and timber member's grain direction; ***ρ***: density of the timber member.

3.2 Cyclic loading protocols

Three different displacement-controlled cyclic loading procedures, which involves displacement cycles grouped in phases at incrementally increasing displacement levels, were adopted to investigate the influence of test protocols on the ductility capacity and the low-cyclic fatigue strength of connections. The load protocols reported in EN12512 [9] and ISO 16670 [23] were adopted at University of Trento (TN) and University of Kassel (KS), respectively. In addition, the load protocols for hold-downs in Kassel took into account the compression part of the studs. A new cyclic load protocol was used in the test campaign carried out at the National Research Council of Italy (CNR) in order to increase the number of steps of the current version of EN12512 [9] after the yielding point, with a higher number of steps in the hysteresis loop on the load-displacement curves and hence a higher accuracy in the analysis process of results.

If the amplitudes of the reversed cycles in ISO 16670 [23] protocol are a function of the ultimate slip obtained from a previous monotonic test $v_{u,m}$, in the EN12512 [9] and CNR protocol the amplitudes of the cycles are defined on the base of the yield slip $v_{y,m}$ determined from a previous monotonic test. The steps and the amplitude of cyclic slips of the three test protocols are reported in Table 5.

Table 5: Amplitude levels of load cycles in terms of the yielding $v_{y,m}$ and ultimate $v_{u,m}$ displacement

Lab.	**Standard**	**Steps**	**1**	**2**	**3**	**4**	**5**	**6**	**7**	**8**	**…**	**n**
KS	ISO 16670	No. of cycles	1	1	1	1	1	3	3	3	…	3
		Amplitude $[v_{u,m}]$	0.0125	0.025	0.05	0.075	0.1	0.2	0.4	0.6	…	(+0.2)
TN	EN12512	No. of cycles	1	1	3	3	3	3	3	3	…	3
		Amplitude $[v_{y,m}]$	0.25	0.50	0.75	1.0	2.0	4.0	6.0	8.0	…	(+2.0)
CNR	CNR protocol	No. of cycles	1	1	3	3	3	3	3	3	…	3
		Amplitude $[v_{y,m}]$	0.2	0.4	0.6	0.8	1.0	1.5	2.0	3.0	…	(+1.0)

3.3 Processing of test data

The methods for the processing of the test data are described in this section. An analytical relationship between the impairment of strength and the slip amplitude was established, firstly; a proposal to take into account the strength degradation in the determination of ultimate slip for the calculation of the ductility capacity is then presented.

The first quadrant of the cycle load-vs-slip curves has been chosen in the processing of test data and in the analysis of results. As an alternative, the same procedure could have been applied to the third quadrant with exception of not fully-reversed load protocols (i.e. hold-down). The most conservative results in the determination of ductility and strength degradation between the curves of the first and the third quadrant could have been adopted in the determination of the low-cycle fatigue strength of connections.

3.3.1 The impairment of strength factor η_{deg} between the 1st and 3rd cycle

The impairment of strength between the 1st and 3rd cycle is defined as the reduction of the load Δ_F when attaining a given slip from the first to the third cycle of the same amplitude v [9]. It can be calculated as reported in eq. 2 as the difference between the loads related the 1st and the 3rd Envelope Load-Slip Curves at the same value of amplitude v, see Figure 5.

$$\Delta_F(v) = F_1(v) - F_3(v) \geq 0 \qquad (2)$$

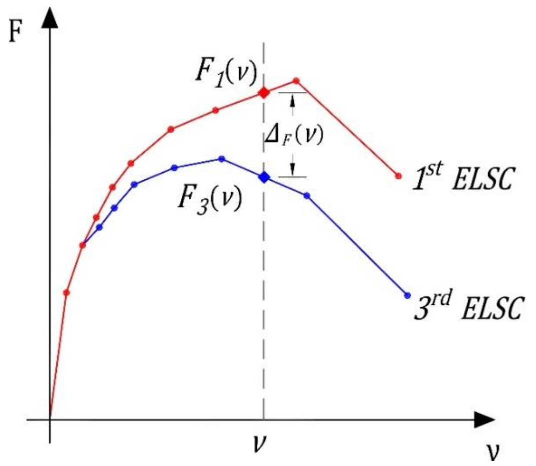

Figure 5: Impairment of strength ΔF(v) between the 1st and 3rd Envelope Load-Slip Curves

The impairment of strength factor $\eta_{deg}(v)$ is introduced in this study as the ratio between the load value related to 3rd cycle $F_3(v)$ and the load related to the 1st cycle $F_3(v)$ at the same slip amplitude v, see eq. 3.

$$\eta_{deg}(v) = \frac{F_3(v)}{F_1(v)} = 1 - \frac{\Delta_F(v)}{F_1(v)} \leq 1 \tag{3}$$

In order to compare different typologies of connections a dimensionless amplitude of slip $\tilde{v}$ is defined in eq.4 as:

$$\tilde{v} = \frac{v}{v_y} \tag{4}$$

where v_y is the yield slip amplitude determined by the procedure reported in EN12512 [9].

The curves η_{deg} vs $\tilde{v}$ have been plotted for all the tested connections. All the curves showed an inverse relationship between η_{deg} and $\tilde{v}$ which, in most cases, can be approximated by a linear interpolation, see Figure 6, for the values of η_{deg} lower than 1. An analytical linear expression between η_{deg} and $\tilde{v}$ can hence be determined in the form reported in eq. 5, for values of slip amplitude lower than the dimensionless ultimate slip $\widetilde{v_u}$

$$\eta_{deg}(\tilde{v}) = a \cdot (\tilde{v} - 1) + \eta_{deg,\tilde{v}=1} \leq 1 \text{ with } \tilde{v} \leq \widetilde{v_u} = \frac{v_u}{v_y} \quad (5)$$

The coefficient a is the slope of the linear interpolating curve and represents the influence of the slip amplitude on the impairment of strength. The parameter $\eta_{deg,\tilde{v}=1}$ is the value of the impairment of strength factor related to a unitary value of the dimensionless slip, namely when $v = v_y$.

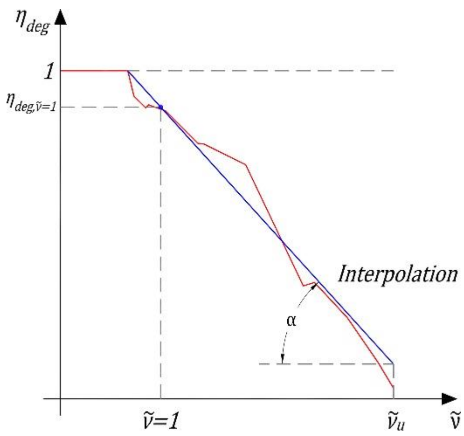

Figure 6: Impairment of strength factor vs dimensionless slip amplitude

3.3.2 Strength degradation as an additional condition for the determination of ductility

In this section a novel methodology to take into account the strength degradation in the determination of ultimate condition of timber connections is presented.

<u>Step 1</u>

The yield and the ultimate slip v_y and v_u are calculated for each test according to the procedures of EN12512 [9], K&Y [28] and ASTM E2126 [2] and discussed in Section 2.2.

<u>Step 2</u>

In order to take into account for the impairment of strength between the 1st and 3rd ELSC in the evaluation of the ultimate condition, the degradation ultimate slip $v_{u,deg}$ is introduced. $v_{u,deg}$ is calculated, see eq.6, as the minimum value between the ultimate slip v_u and the value of displacement related to a certain limit value of the impairment of strength factor, $\eta_{deg,lim} \epsilon [0;1]$.

$$v_{u,deg} = \min\left[v_u; v(\eta_{deg} = \eta_{deg,lim})\right] \quad (6)$$

For connections with a significant impairment of strength, $v(\eta_{deg} = \eta_{deg,lim})$ will be lower than v_u, and as a result $v_{u,deg} = v\left(\eta_{deg} = \eta_{deg,lim}\right) < v_u$, see Figure 7a. For connections with low impairment of strength, v_u will be lower than $v(\eta_{deg} = \eta_{deg,lim})$, and therefore $v_{u,deg} = v_u < v\left(\eta_{deg} = \eta_{deg,lim}\right)$, Figure 7b.

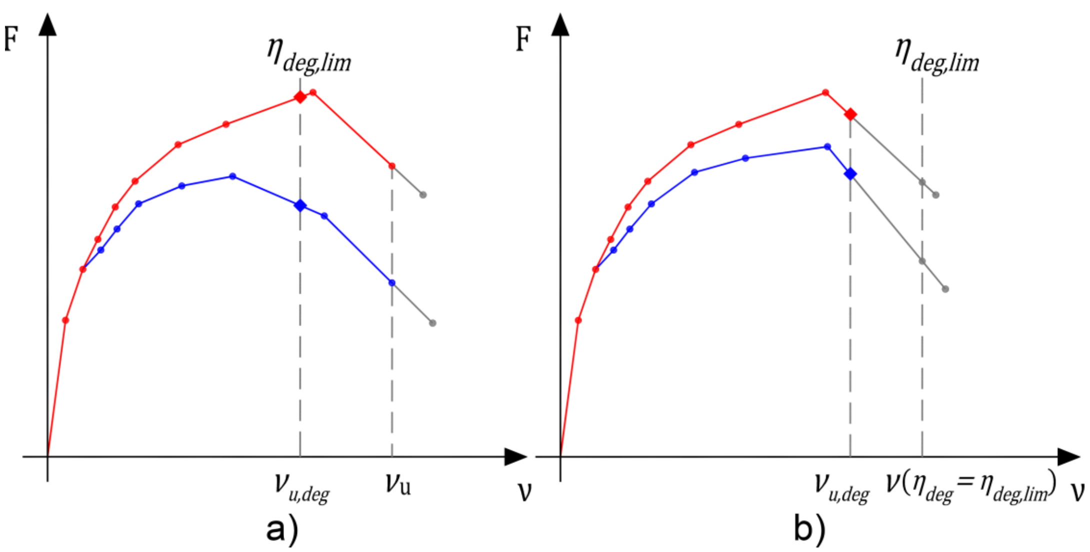

Figure 7: Determination of the degradation ultimate slip $v_{u,deg}$

<u>Step 3</u>

In order to ensure that the connection exhibits for all the values of amplitudes up to $v_{u,deg}$ a cyclic strength capacity not significantly lower than the nominal strength F_N, a lowest limit value for the 1st cycle load $F_1(v)$ is introduced.

Similarly to the method reported in ANSI/AISC 341-10 [3] for steel beam-to-column joints, this study proposes that the ratio $\tilde{f}_{deg}$ between the 1st ELSC F_1 at a slip amplitude $v_{u,deg}$ and the nominal strength $F_{N,}$ is equal or higher than a certain limit value $\tilde{f}_{deg,lim}$ as reported in eq.7

and shown in Figure 8a. In this paper, the nominal strength F_N has been determined as the maximum value of load obtained from previous monotonic tests for values of the slip lower than 15 mm according to EN26891 [10].

$$\tilde{f}_{deg}(v_{u,deg}) = \frac{F_1(v_{u,deg})}{F_N} \geq \tilde{f}_{deg,lim} \tag{7}$$

When eq. 7 is not satisfied, the degradation ultimate displacement v_{deg} is reduced to a lower value of slip able to satisfy eq. 7, see Figure 8b. If eq. 7 is not satisfied for any other value of slip, as in the case of Figure 8c, the connection should not be used for dissipative connections.

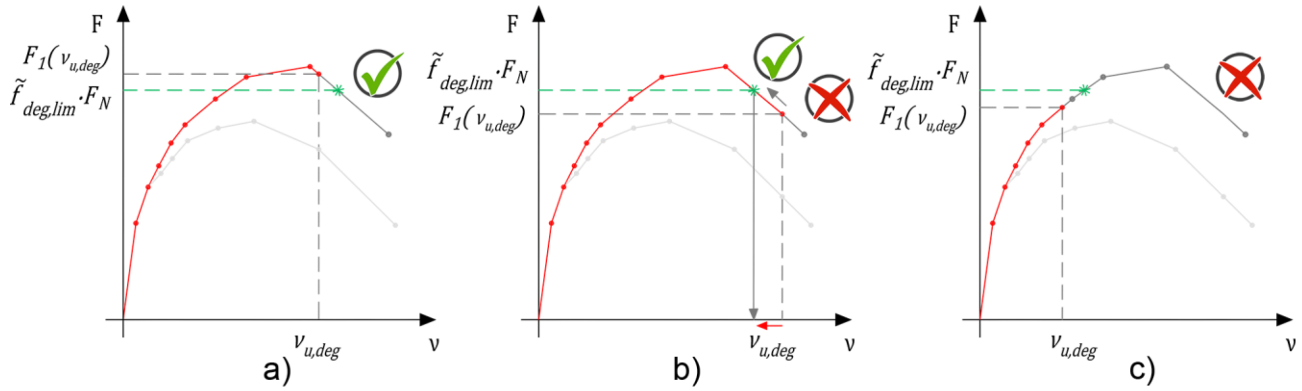

Figure 8: Verification of the cyclic strength related to the 1st ELSC; eq. 7 satisfied at the value of $v_{u,deg}$ calculated from eq.6, a); eq. 7 satisfied at the value of slip amplitude lower than the value of $v_{u,deg}$ calculated from eq.6, b); eq.7 not satisfied for any value of slip amplitude c)

<u>Step 4</u>

Finally, the ductility capacity has been calculated according to eq. 8 as the ratio between the degradation ultimate slip $v_{u,deg}$ and the yield slip v_y determined from procedures reported in Section 2.2 and shown in Figure 9.

$$\mu_{deg} = \frac{v_{u,deg}}{v_y} \tag{8}$$

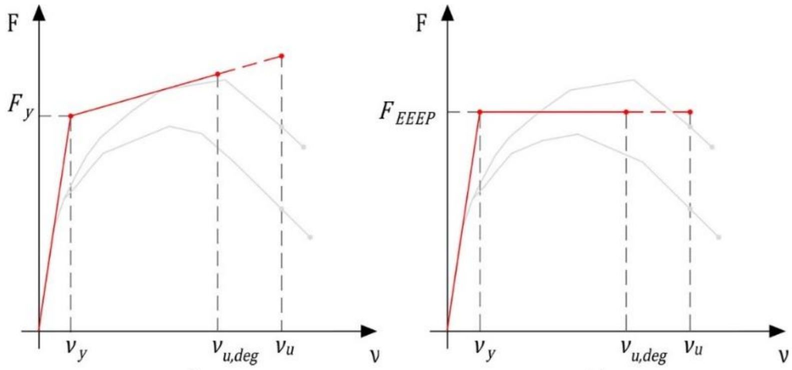

a) b)

Figure 9: Yield slip and degradation ultimate slip on the elastic-plastic curves determined according to EN12512 [9] (a) and ASTM E2126 [2]/ K&Y [28] (b)

4. Results and Discussion

4.1 Determination of the impairment of strength factor η_{deg}

According to the procedure reported in Section 3.3.1 the impairment of strength factor η_{deg} has been determined for all the tested connections as a function of the dimensionless slip amplitude $\tilde{v}$ from eq. 3. The coefficients a, $\eta_{deg,\tilde{v}=1}$ and $\widetilde{v_u}$ are reported for all the tests in Table 6-to-9. The failure mode for each test was added into the tables. In Figure 10 and Figure 11 the test set-up and the results for tests SC_CLT_1, SC_CLT_2, HD_AN_1 and HD_AN_8 are shown.

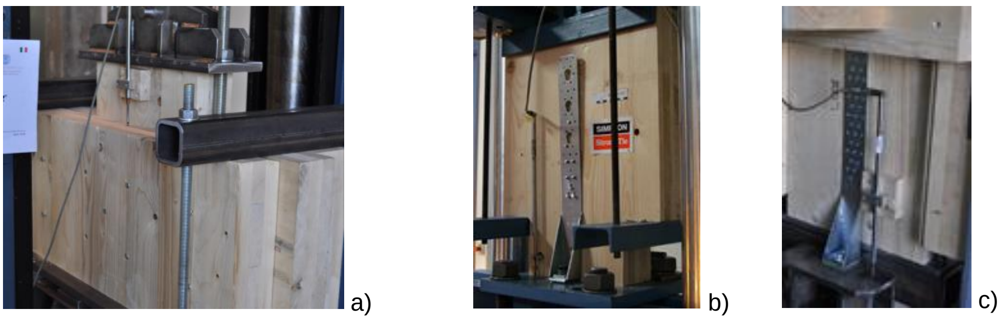

Figure 10: Cyclic tests SC_CLT_1 and SC_CLT_2, a), HD_AN_1, b), and HD_AN_8, c)

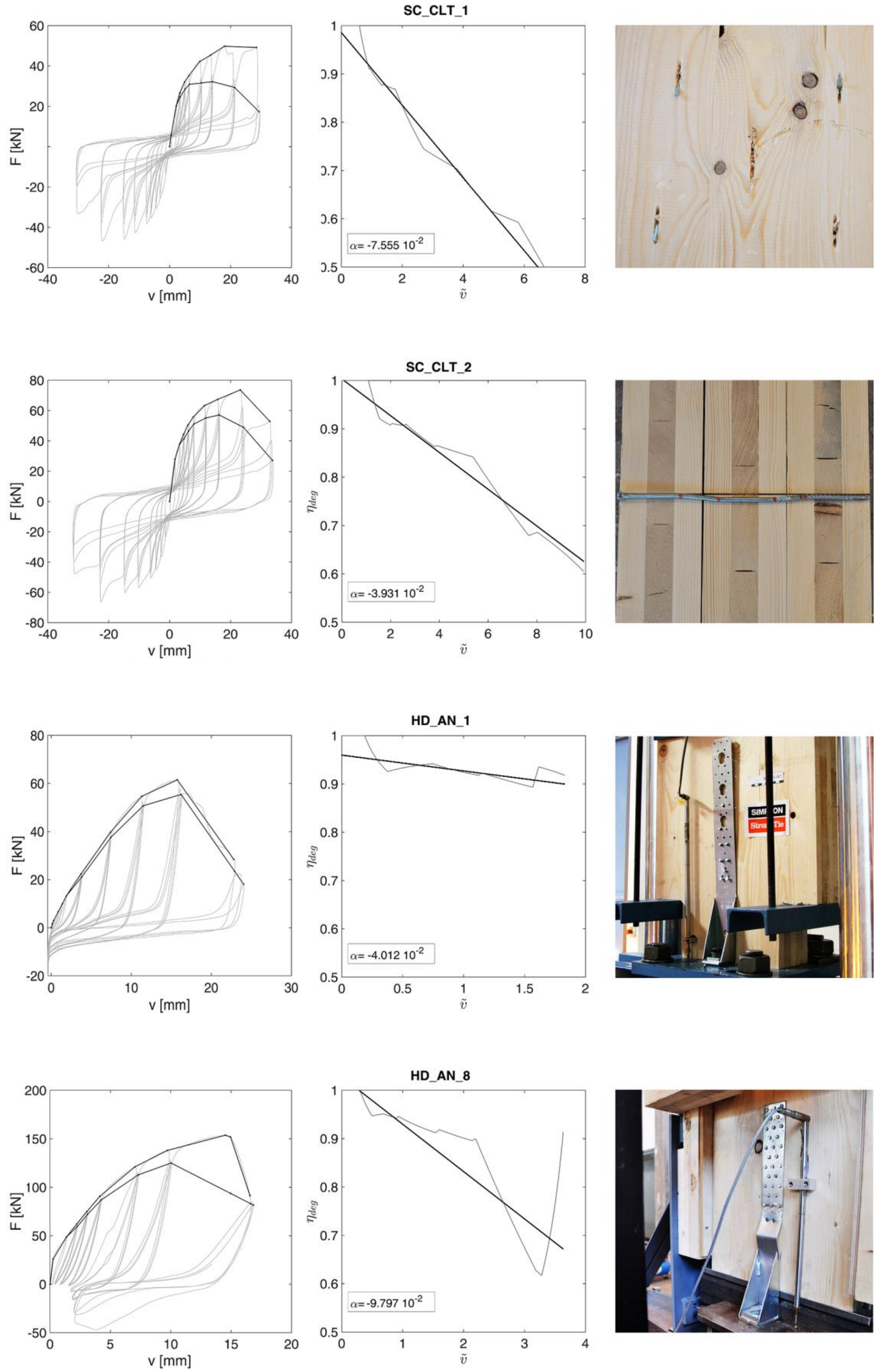

Figure 11: Cyclic tests on screwed connection, tests SC_CLT_1, SC_CLT_2, HD_AN_1, and HD_AN_8

The η_{deg}- $\tilde{v}$ linear curves are reported in Figure 12 for P2T connections. Ring nails (RN) showed a higher impairment of strength than smooth nails when OSB panels were used: a mean value of the coefficient a *(10^{-2})* equal to -6.70 and -3.38 was obtained from the tests RN_OSB_1-to-4 and SN_OSB_1-to-3, respectively. A large scattering of the interpolating linear curves was observed for stapled connections, see Figures 12c and 12d. The lowest value of the coefficient a *(10^{-2})* was equal to -11.63 and -12.84 for the tests ST_OSB_3 and ST_GFB_3, respectively, whereas the highest value was equal to -0.57 and -1.57 for the tests ST_OSB_2 and ST_GFB_2.

An average value of the coefficient $\eta_{deg,\tilde{v}=1}$ equal to 0.96 was obtained for RN P2T connections, showing a negligible impairment of strength for values of slip amplitude lower than the yield displacement. An average value of the coefficient $\eta_{deg,\tilde{v}=1}$ equal to 0.86 was conversely calculated for staples with GFB panel.

For P2T connections the failure mode was different depending on the fastener type and sheathing material. Ring nails and smooth nails showed plastic hinges in all cases. Staples showed either fatigue failure or plastic hinges. According to the failure modes, the P2T connections with nails, in average, showed values of the ultimate dimensionless slip $\widetilde{\boldsymbol{v}_{\boldsymbol{u}}}$ 50 % higher than P2T stapled connections.

For tests SN_OSB_1, SN_OSB_2, SN_GFB_1 a coefficient $\eta_{deg,\tilde{v}=1}$ higher than 1 was obtained. It is noteworthy to mention that the values of the coefficient $\eta_{deg,\tilde{v}=1}$ higher than 1 do not have a physical meaning since the impairment of strength is to be lower or equal than 1 according to eq. 5. The values of the coefficient $\eta_{deg,\tilde{v}=1}$ are used to define the analytical relationship between the impairment of strength factor and the dimensionless slip amplitude.

Table 6: Coefficient for the linear relationship between the impairment of strength factor η_{deg} and the dimensionless slip amplitude $\widetilde{v_u}$ for P2T connections

P2T Connections	a (10^-2)	$\eta_{deg,\tilde{v}=1}$	$\widetilde{v_u}$	Failure mode
RN_OSB_1	-8.14	0.9672	8.57	Plastic hinges in the nails
RN_OSB_2	-6.49	0.9511	7.26	Plastic hinges in the nails
RN_OSB_3	-6.12	0.9774	13.79	Plastic hinges in the nails
RN_OSB_4	-6.05	0.9470	6.66	Plastic hinges in the nails
SN_OSB_1	-3.27	1.0495	12.72	Plastic hinges in the nails
SN_OSB_2	-4.19	1.1298	16.50	Plastic hinge and pull out of the nails
SN_OSB_3	-2.67	0.9751	21.19	Plastic hinges in the nails
SN_GFB_1	-7.06	1.088	11.07	Plastic hinge and pull out of the nails
ST_OSB_1	-5.93	0.9436	7.19	Plastic hinges in the staples
ST_OSB_2	-0.57	0.955	12.82	Fatigue failure of staples
ST_OSB_3	-11.63	0.8347	5.89	Fatigue failure of staples
ST_GFB_1	-6.83	0.8095	6.08	Fatigue failure of staples
ST_GFB_2	-1.57	0.8939	11.72	Pull out of staples and crack in GFB
ST_GFB_3	-12.84	0.9193	6.36	-

The low-cycle behaviour of T2T connections, see Table 7 and Figure 13, showed a large dependency on the diameter of screws, confirming the results reported in Izzi & Polastri [25]. In case of 6 mm screws, a significant impairment of strength was detected for low amplitude plastic deformations with values of the coefficient a *(10^{-2})* equal to -13.63, -14.40 and -7.55 for tests SC_GLT_1, SC_GLT_2 and SC_CLT_1 and an ultimate dimensionless slip amplitude $\widetilde{v_u}$ lower than 4.11 for the tests SC_GLT_1 and SC_GLT_2. A good cycle fatigue strength was, conversely, observed for 10 mm screws with values of the coefficient a *(10^{-2})* equal to -3.09, -2.10 and -0.35 for the test SC_GLT_5, SC_GLT_6 and SC_CLT_3 and values of $\widetilde{v_u}$ higher than 6.79. An average value of $\eta_{deg,\tilde{v}=1}$ equal to 0.96 was calculated for all screwed T2T connections. A negligible strength degradation was observed for the dowelled connection, i.e. D_CLT_1, with a quasi-constant value of η_{deg} approximately equal to 0.95 for any value of dimensionless slip amplitude.

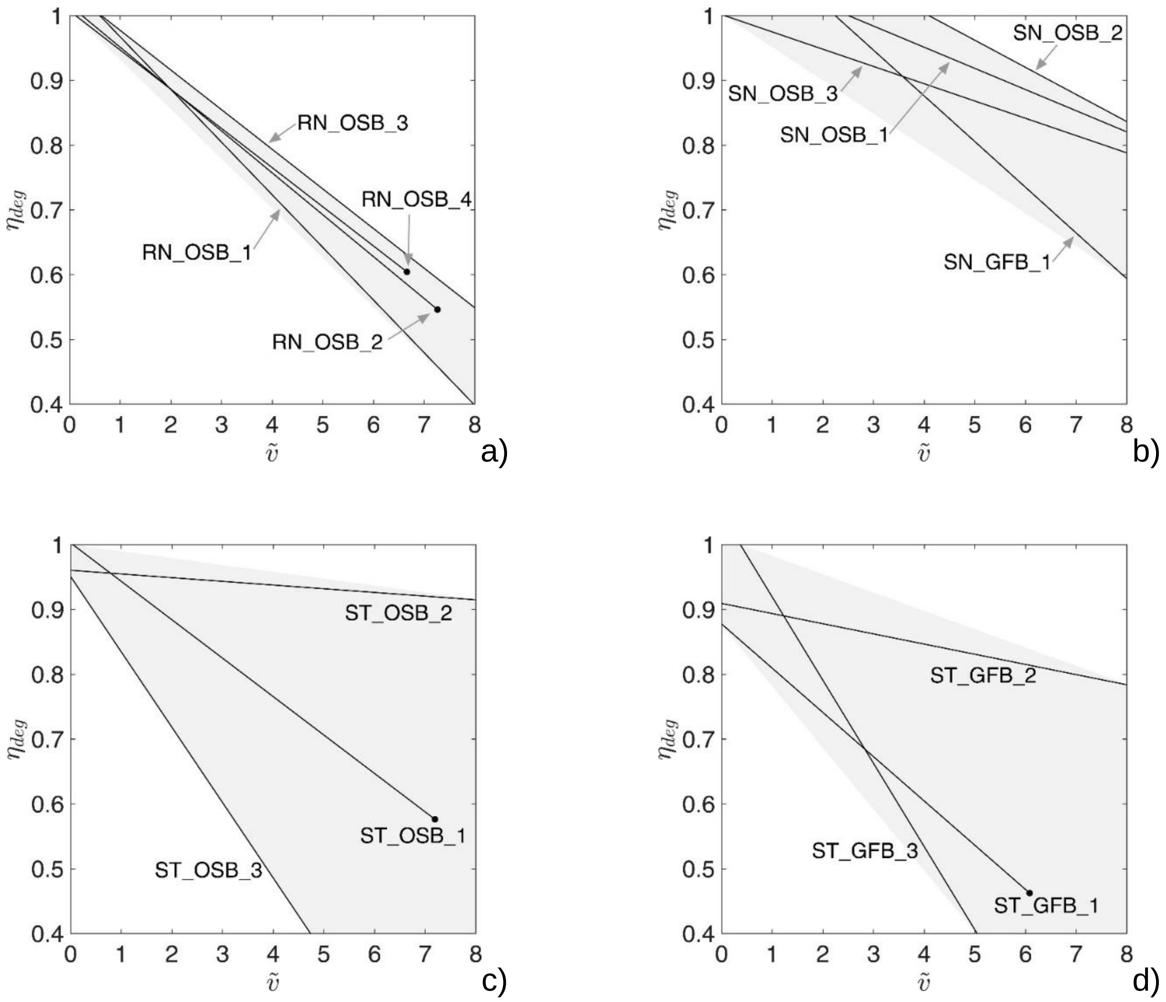

Figure 12: Impairment of strength factor vs dimensionless slip curves for the P2T connections; a) ring nailed OSB panel-to-timber connection; b) smooth nailed OSB/GFB panel-to-timber connection; c) stapled OSB panel-to-timber connection; d) stapled GFB panel-to-timber connection

The failure mode of T2T connections showed a strong dependency on the fastener diameter. Increasing the diameter from 6mm to 10mm, the T2T connections with GLT move from failure modes due to cyclic fatigue to failure modes which involve high rotations of plastic hinges in the fasteners. The same behaviour was observed for T2T connections with CLT members. In accordance to the observed failure modes, the dimensionless ultimate slip for T2T connections increased changing the failure mode from fatigue failure to plastic hinges failure and with increasing the fastener diameter.

Table 7: Coefficient for the linear relationship between the impairment of strength factor η_{deg} and the dimensionless slip amplitude $\widetilde{v_u}$ for T2T connections

T2T Connections	a (10^{-2})	$\eta_{deg,\tilde{v}=1}$	$\widetilde{v_u}$	Failure mode
SC_GLT_1	-13.63	0.9342	4.11	Fatigue failure of screws
SC_GLT_2	-14.40	0.8979	3.22	Fatigue failure of screws
SC_GLT_3	-6.91	0.9295	4.65	Fatigue failure of screws
SC_GLT_4	-5.07	0.9567	9.05	Plastic hinges in screws
SC_GLT_5	-3.09	0.9315	7.04	Plastic hinges in screws
SC_GLT_6	-2.10	0.9032	6.79	Plastic hinges in screws
SC_CLT_1	-7.55	0.9102	7.74	Fatigue failure of screws
SC_CLT_2	-3.93	0.9671	9.89	Plastic hinges in screws
SC_CLT_3	-0.35	0.9088	11.30	Plastic hinges in screws
D_CLT_1	-0.03	0.9425	14.03	Plastic hinges in dowels

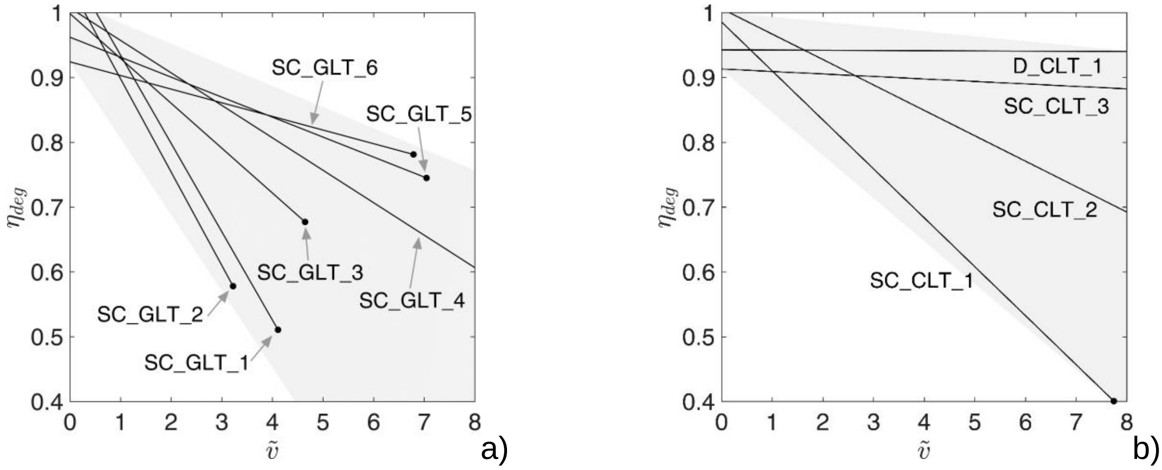

Figure 13: Impairment of strength factor vs dimensionless slip curves for the T2T connections; a) screwed glulam-to-glulam connection; b) screwed and dowelled CLT-to-CLT connection

The impairment of strength factor was higher than 0.8, see Figure 14, for any value of the dimensionless slip amplitude for tests on S2T connections; values of the coefficient a *(10^{-2})* from -3.18 to -2.61 for AN connections and from -4.82 and -2.08 for SC connections have been calculated. The linear curves of impairment of strength factor are limited in a small region showing a low scattering of results. However, values of of $\widetilde{v_u}$ not higher than 4.01 and 2.69 were achieved for nailed and screwed connection, respectively, showing a limited capacity to undergo medium-to-high plastic deformation.

For S2T connections the failure mode was due to the head failure in all cases. Despite this similitude in the failure modes, S2T connections with annular ringed nails reached values of the ultimate dimensionless slip $\widetilde{\boldsymbol{v_u}}$ averagely 80% higher than S2T connections with screws.

Table 8: Coefficient for the linear relationship between the impairment of strength factor $\boldsymbol{\eta_{deg}}$ and the dimensionless slip amplitude $\widetilde{v_u}$ for S2T connections

S2T Connections	a (10^{-2})	$\eta_{deg,\tilde{v}=1}$	$\widetilde{v_u}$	Failure mode
AN_S_3	-2.61	0.9119	3.90	tear-off failure of the head
AN_S_1	-3.18	0.9359	3.67	tear-off failure of the head
AN_S_2	-2.45	0.9239	4.01	tear-off failure of the head
SC_S_3	-4.82	0.9230	2.08	tear-off failure of the head
SC_S_1	-3.10	0.9272	2.69	tear-off failure of the head
SC_S_2	-2.08	0.9098	1.68	tear-off failure of the head

A significant scattering of results was observed for hold downs tests, HD_AN_01-to-08, as shown in Figure 15. For the tests HD_AN_1 and HD_AN_5, characterized by values of $\widetilde{v_u}$ lower than 2, values of η_{deg} higher than 0.85 were obtained; the failure of the connection was achieved for low amplitude plastic deformations; a negligible impairment of strength was for this reason observed. A value of the coefficient a *(10^{-2})* equal to -4.01 and -4.83 was obtained, respectively. For tests HD_AN_6 and HD_AN_8, the hold-down were able to achieve a value of $\widetilde{v_u}$ equal to 2.43 and 3.31; a higher strength degradation than the tests HD_AN_1 and HD_AN_5 was observed, with a value of *a (10^{-2})* equal to -13.1 for the test HD_AN_6.

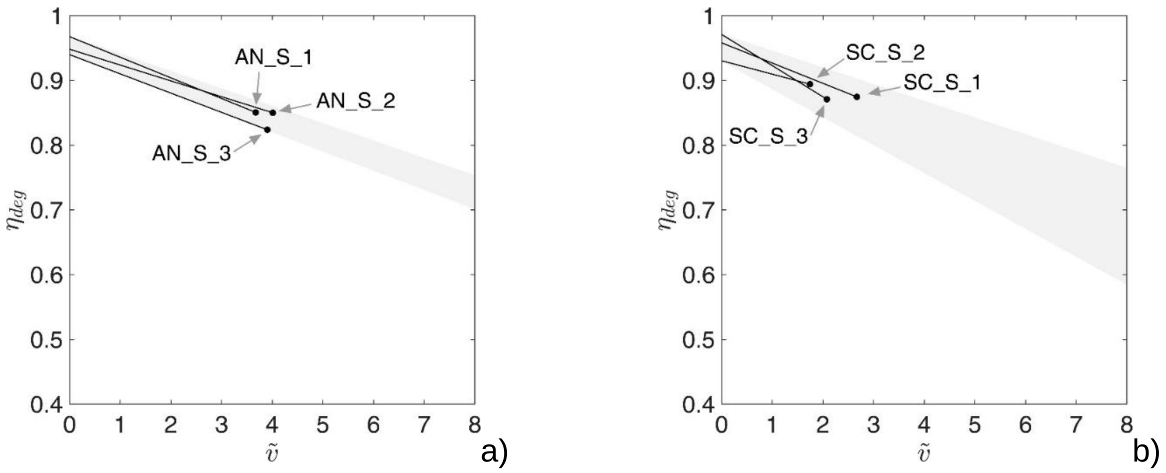

Figure 14: Impairment of strength factor vs dimensionless slip curves for the S2T connections; Anker nailed connection a); screwed connection, b).

A low-cycle fatigue strength and low capacity to undergo plastic deformation was observed for all the three angle brackets' tests with values of the coefficient a *(10^{-2})* up to -24.39 and values of $\widetilde{v_u}$ not higher than 2.03.

MA connections showed different failure modes. Hold-downs with an overstrength in the metal steel plate showed a failure mode in the fasteners with plastic hinges. On the contrary, fully nailed hold-downs showed a brittle steel plate failure. Hold-downs with an interlayer showed a failure mode with plastic hinges in the fasteners. MA with angle brackets showed different failure modes depending on the support element. Angle brackets with timber supporting, AB_2 and AB_3, element showed failure modes with plastic hinges in the nails. Angle bracket with steel supporting element, AB_1, showed a failure of the bolts used to anchor the angle bracket to the steel beam.

MA connections which exhibited failure with plastic hinges in the fasteners (HD_AN_1 to 3) reached averagely values of $\widetilde{v_u}$ about 35% higher than MA connections with failure in the steel plate (HD_AN_4 to 8).

Table 9: Coefficient for the linear relationship between the impairment of strength factor η_{deg} and the dimensionless slip amplitude $\widetilde{v_u}$ for MA connections

MA Connections	a (10-2)	$\eta_{deg,\tilde{v}=1}$	$\widetilde{v_u}$	Failure mode
HD_SC_1	-0.19	0.9297	2.36	tear-off failure of the head
HD_AN_1	-4.01	0.9245	1.86	Plastic hinges and pull out of nails
HD_AN_2	-12.60	0.9406	3.98	Plastic hinges
HD_AN_3	-7.97	0.9423	3.00	Plastic hinges
HD_AN_4	-4.93	0.9720	1.71	Steel plate tensile load failure
HD_AN_5	-4.83	0.9781	1.75	Steel plate tensile load failure
HD_AN_6	-13.10	0.8788	2.43	Steel plate tensile load failure
HD_AN_7	-9.32	0.9153	1.64	Steel plate tensile load failure
HD_AN_8	-8.13	0.9298	3.35	Steel plate tensile load failure
HD_OSB_1	-4.17	0.9571	3.72	Plastic hinges and pull out of nails
HD_GFB_1	-5.31	0.9216	4.01	Plastic hinges and pull out of nails, tear out of GFB
AB_1	-12.75	0.8362	1.13	Failure of bolts used to anchor the AB
AB_2	-20.24	0.8785	2.03	Plastic hinges and pull out of nails
AB_3	-24.39	0.8410	1.67	Plastic hinges and pull out of nails

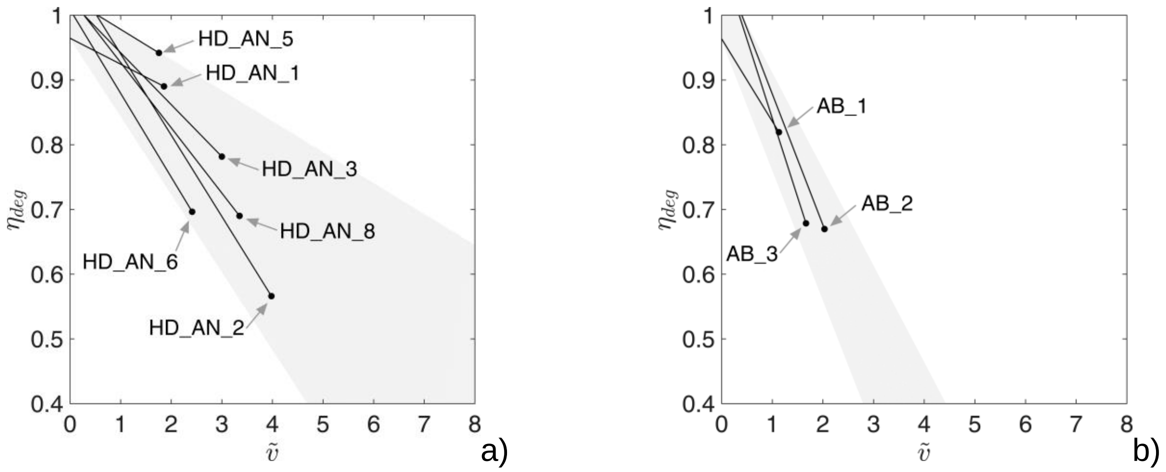

Figure 15: Impairment of strength factor vs dimensionless slip curves for the MA connections; a) hold-downs; b) angle brackets

4.2 Ductility capacity and strength degradation

Different limit values of the impairment of strength factor $\eta_{deg,lim}$ between 0.5 and 0.9 were selected to take into account the influence of strength degradation on ductility capacity μ_{deg} according to eq. 6 and 8. The additional case which the strength degradation was not considered in the calculation of $v_{u,deg}$ was chosen as well, setting $\eta_{deg,lim}$ equal to zero, i.e.

without (w/o) $\eta_{deg,lim}$.

The procedures reported EN 12512 [9], ASTM E2126 [2] and K&Y [28] were adopted to determine the yield displacement v_y in eq. 8. A limit value of $\tilde{f}_{deg,lim}$ equal to 0.8 was fixed for the condition expressed by eq. 7.

In Tables 10 to 13 the values of μ_{deg} and $\tilde{f}_{deg}$ are reported for all four categories of connections for the cases without (w/o) considering $\eta_{deg,lim}$ and $\eta_{deg,lim} = 0.7$ and $\eta_{deg,lim} = 0.8$ (this value corresponds to the authors' interpretation of considering a limit the value of impairment of strength equal to 20% in the current version of the Eurocode 8 [11]).

When the condition of eq. 7 was satisfied by reducing the value of the degradation ultimate slip $v_{u,deg}$ the symbol (*) was adopted in Tables 10 to 13, see Figure 8b. The symbol (**) was used for tests which eq. 7 was not satisfied for, at any value of $v_{u,deg}$, see, Figure 8c.

For P2T connections, a significant influence of strength degradation in the determination of the ductility capacity was observed. For all tests, in fact, with exception of ST_OSB_2, the values of ductility capacity calculated considering a limit value of the impairment of strength equal to 0.8 are significantly lower than the case which the strength degradation is not taken into account for, see Table 10. In Figure 16 the values μ_{deg} for the tests RN_OSB_4, SN_OSB_1, ST_GFB_2 and ST_OSB_1 are plotted as function of $\eta_{deg,lim}$. Ring nails and smooth nailed OSB-to-wood connections exhibit a mean value of ductility equal to 4.48 and 8.12, respectively, for $\eta_{deg,lim} = 0.8$ and the EN12512 [9] procedure. Values of ductility not higher than 3.30 are shown by using the same procedure for stapled connection with exception of tests ST_OSB_2 and ST_GFB_2 which, however, the condition of eq. 7 has not been satisfied for. The highest values of ductility are achieved in most cases with the EN12512 [9] procedure whereas the lowest values are obtained for the procedure reported in K&Y [28].

Table 10: Ductility μ_{deg} and $\tilde{f}_{deg}$ factor for P2T connections

P2T connection	μ_{deg}									$\tilde{f}_{deg}$	
	EN 12512			**ASTM E2126**			**K&Y**				
	w/o $\eta_{deg,lim}$	$\eta_{deg,lim}$ =0.7	$\eta_{deg,lim}$ =0.8	w/o $\eta_{deg,lim}$	$\eta_{deg,lim}$ =0.7	$\eta_{deg,lim}$ =0.8	w/o $\eta_{deg,lim}$	$\eta_{deg,lim}$ =0.7	$\eta_{deg,lim}$ =0.8	w/o $\eta_{deg,lim}$	$\eta_{deg,lim}$ =0.8
RN_OSB_1	8.57	5.94	4.29**	5.87	4.07	2.94**	4.14	2.87	2.07**	0.95	0.75
RN_OSB_2	7.26	5.46	4.94	5.42	4.08	3.69	4.01	3.01	2.73	0.89	0.86
RN_OSB_3	10.68*	5.87	4.61	6.95*	3.82	3.00	4.64*	2.55	2.00	0.80	0.83
RN_OSB_4	6.66	5.24	4.08	5.12	4.03	3.14	4.08	3.21	2.50	1.05	1.02
SN_OSB_1	12.72	8.76	6.20	8.71	6.00	4.24	6.96	4.79	3.39	0.90	1.04
SN_OSB_2	16.50	11.26	9.15	9.30	6.35	5.16	5.34	3.65	2.96	1.27	1.12
SN_OSB_3	17.49**	17.49	11.81	12.43**	12.43	8.40	9.85**	9.85	6.65	0.74	0.90
SN_GFB_1	11.07	6.44	5.31	8.06	4.69	3.87	6.44	3.75	3.09	0.90	1.03
ST_OSB_1	7.19*	5.04	3.30	6.19*	4.34	2.84	4.03*	2.83	1.85	0.80	0.94
ST_OSB_2	12.82**	12.82**	12.82**	9.42**	9.42**	9.42**	9.23**	9.23**	9.23**	0.54	0.54
ST_OSB_3	4.96*	1.92**	1.52**	4.29*	1.66**	1.31**	4.07*	1.58**	1.25**	0.80	0.61
ST_GFB_1	4.42*	1.72	1.41**	4.68*	1.82	1.49**	4.66*	1.81	1.48**	0.80	0.72
ST_GFB_2	11.72**	11.72**	4.76**	8.36**	8.36**	3.39**	6.86**	6.86**	2.78**	0.53	0.62
ST_GFB_3	4.34*	2.98**	1.75**	3.80*	2.61**	1.53**	2.56*	1.76**	1.03**	0.80	0.59

(*) condition of eq. 7 satisfied by reducing the value of the degradation ultimate slip $v_{u,deg}$

(**) condition of eq. 7 not satisfied

For T2T screwed connection, a significant difference in terms of ductility capacity and strength degradation was observed dependently on the screws' diameter. 6 mm diameter screws in tests SC_GLT_1-2 and SC_CLT_1, showed a significant influence of the strength degradation in the calculation of the ductility. A large difference between the values of μ_{deg} evaluated without considering the $\eta_{deg,lim}$ and the case where a limit value of $\eta_{deg,lim}$ equal to 0.8 was observed for all the three different Standard procedures. In SC_GLT_1 the value of μ_{deg} drops from 3.90 to 2.31, see Figure 13, for values of $\eta_{deg,lim}$ equal to 0.5 to 0.8, according to EN 12512 [9]. 10 mm screws in tests, SC_GLT_5-6 and SC_CLT_3, showed large values of ductility, not lower than 5.51 for EN12512 [9] procedure, with a limited influence of the strength degradation. As shown in Figure 17 for the test SC_GLT_6, a quasi-constant value of μ_{deg} was achieved for values of $\eta_{deg,lim}$ lower than 0.80.

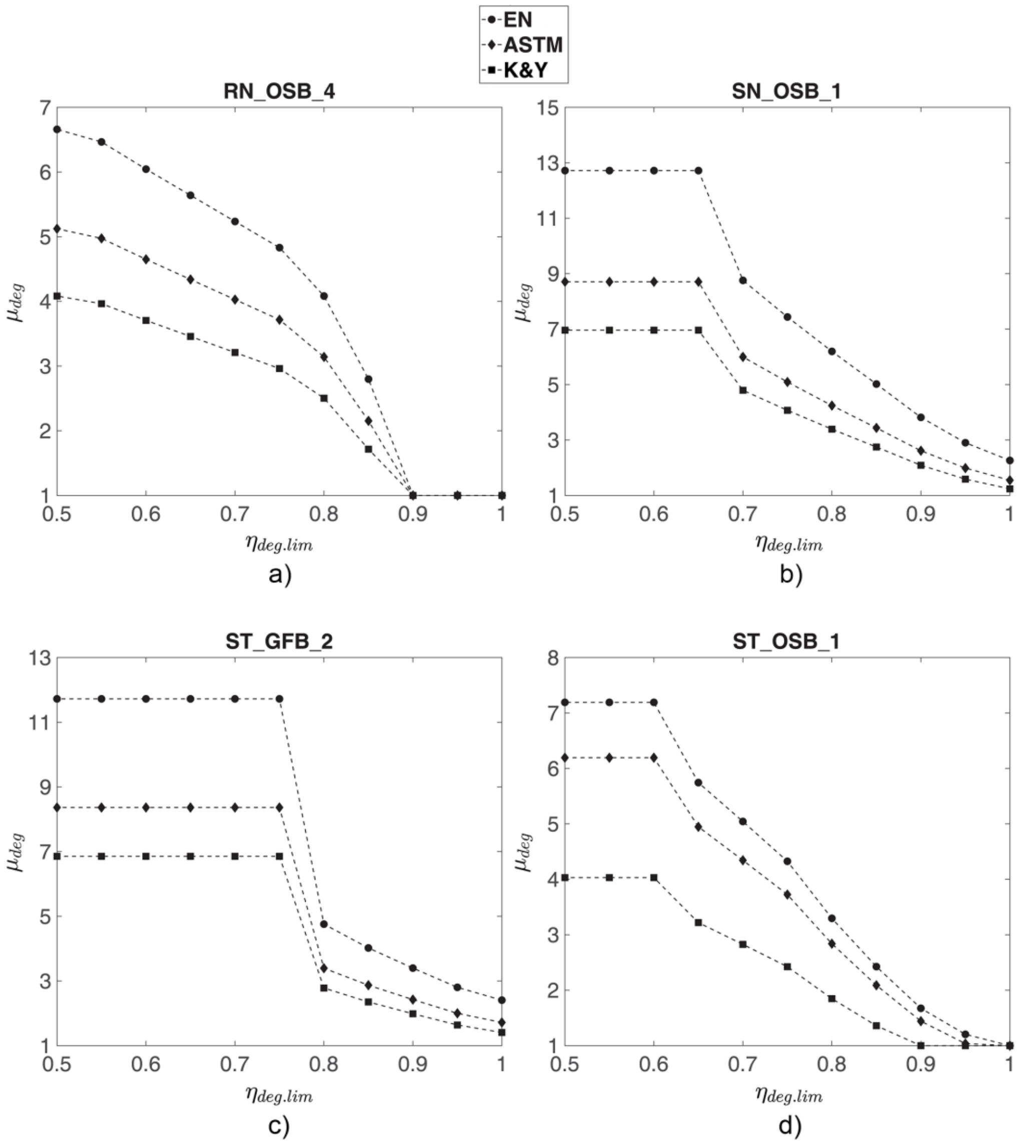

Figure 16: μ_{deg} vs $\eta_{deg,lim}$ curves for tests RN_OSB_4, SN_OSB_1, ST_GFB_2 and ST_OSB_1 ($\tilde{f}_{deg,lim} = 0.8$)

From the the test on dowelled T2T connection, D_CLT_1, costant values of μ_{deg} were obtained for $\eta_{deg,lim}$ between 0.5 and 0.9. The tests showed a negligible impairment of strength between the 1st and the 3rd cycle for high-amplitude plastic deformation with values of ductility higher than 12.56 as shown in Figure 17.

Table 11: Ductility μ_{deg} and $\tilde{f}_{deg}$ factor for T2T connections

T2T connection	μ_{deg}									$\tilde{f}_{deg}$	
	EN 12512			ASTM E2126			K&Y				
	w/o $\eta_{deg,lim}$	$\eta_{deg,lim}$ =0.7	$\eta_{deg,lim}$ =0.8	w/o $\eta_{deg,lim}$	$\eta_{deg,lim}$ =0.7	$\eta_{deg,lim}$ =0.8	w/o $\eta_{deg,lim}$	$\eta_{deg,lim}$ =0.7	$\eta_{deg,lim}$ =0.8	w/o $\eta_{deg,lim}$	$\eta_{deg,lim}$ =0.8
SC_GLT_1	4.11	2.79	2.31	3.76	2.55	2.11	3.25	2.21	1.83	1.02	0.95
SC_GLT_2	3.22	2.32	1.83	3.06	2.21	1.73	2.36	1.70	1.34	1.16	0.93
SC_GLT_3	4.64	4.47	2.82	3.98	3.83	2.42	3.10	2.98	1.88	1.15	1.01
SC_GLT_4	9.05	6.33	4.40	6.11	4.27	2.97	4.81	3.37	2.34	1.33	1.13
SC_GLT_5	7.04	7.03	5.51	5.70	5.68	4.45	3.73	3.72	2.91	0.97	0.94
SC_GLT_6	6.79	6.79	6.79	6.05	6.05	6.05	3.95	3.95	3.95	0.93	0.93
SC_CLT_1	7.74	3.82	2.23	5.89	2.91	1.70	4.69	2.32	1.00	1.00	0.79
SC_CLT_2	9.89	7.32	5.91	7.03	5.19	4.19	4.76	3.53	2.84	0.91	1.06
SC_CLT_3	11.30	11.30	9.59	9.21	9.21	7.81	6.35	6.35	5.39	0.87	1.03
D_CLT_1	14.03	14.03	14.03	14.04	14.04	14.04	12.56	12.56	12.56	1.02	1.02

(*) condition of eq. 7 satisfied by reducing the value of the degradation ultimate slip $v_{u,deg}$

(**) condition of eq. 7 not satisfied

With exception of test AN_S_3, S2T connections showed a negligible influence of the impairment of strength factor on the assessment of the ductility capacity, see Figure 18. Values of μ_{deg} not higher than 4.01 and 2.67 were determined for Anker nailed and screwed connections, respectively, according to the procedure of EN12512 [9] and with $\eta_{deg,lim} = 0.8$. In all tests, the condition reported in eq.7 was satisfied without any reduction of the degradation ultimate displacement.

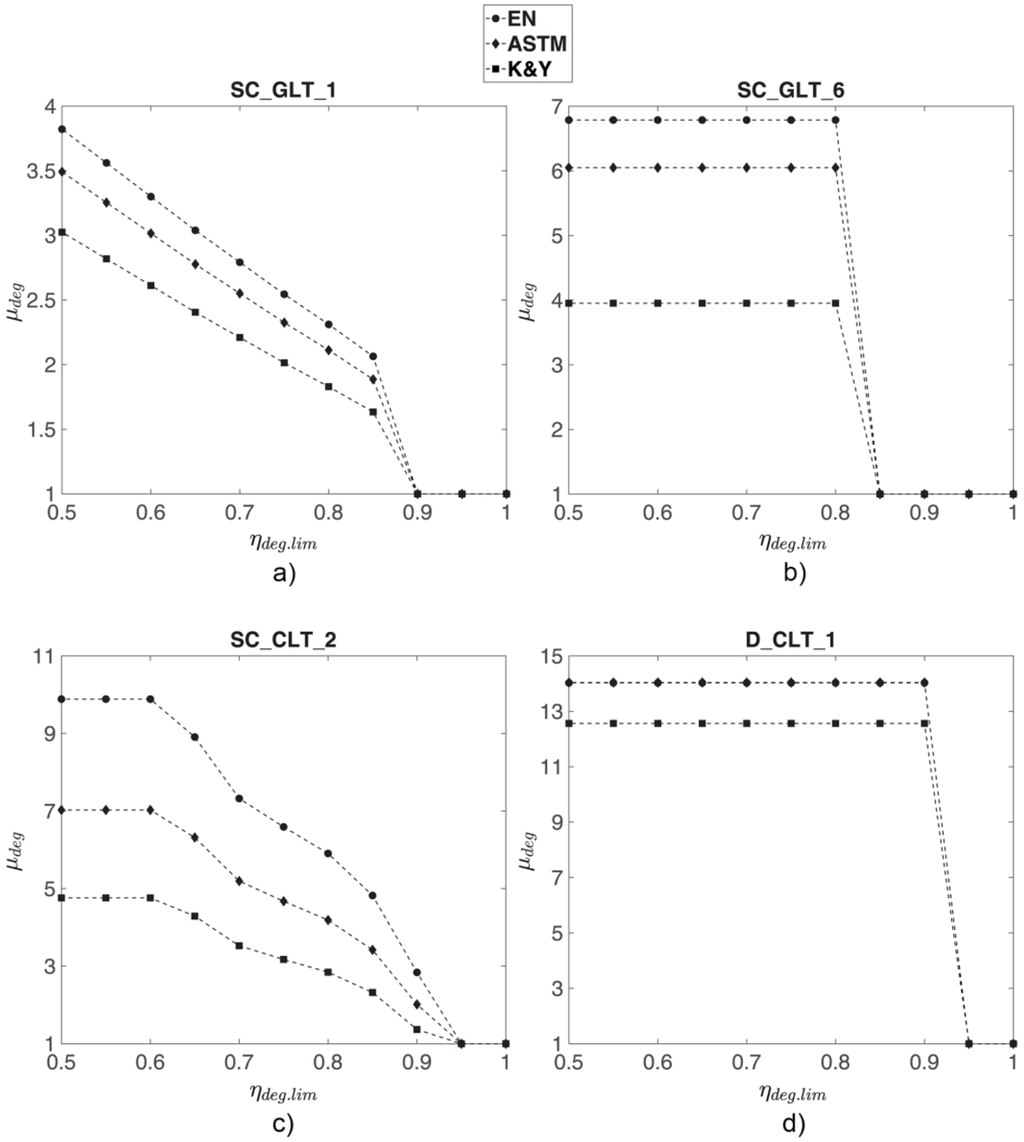

Figure 17: μ_{deg} vs $\eta_{deg,lim}$ curves for tests SC_GLT_1, SC_GLT_6, SC_CLT_2 and D_CLT_1 ($\tilde{f}_{deg,lim} = \mathbf{0.8}$)

Table 12: Ductility μ_{deg} and $\tilde{f}_{deg}$ factor for S2T connections

S2T connection	μ_{deg}									$\tilde{f}_{deg}$	
	EN 12512			ASTM E2126			K&Y				
	w/o $\eta_{deg,lim}$	$\eta_{deg,lim}$ =0.7	$\eta_{deg,lim}$ =0.8	w/o $\eta_{deg,lim}$	$\eta_{deg,lim}$ =0.7	$\eta_{deg,lim}$ =0.8	w/o $\eta_{deg,lim}$	$\eta_{deg,lim}$ =0.7	$\eta_{deg,lim}$ =0.8	w/o $\eta_{deg,lim}$	$\eta_{deg,lim}$ =0.8
AN_S_1	3.67	3.67	3.67	3.56	3.56	3.56	2.91	2.91	2.91	1.01	1.01
AN_S_2	4.01	4.01	4.01	4.20	4.20	4.20	3.74	3.74	3.74	0.87	0.87
AN_S_3	3.90	3.90	1.44	4.22	4.22	1.56	3.73	3.73	1.38	-	-
SC_S_1	2.67	2.67	2.67	2.81	2.81	2.81	2.35	2.35	2.35	1.04	1.04
SC_S_2	1.68	1.68	1.68	2.10	2.10	2.10	1.73	1.73	1.73	0.96	0.96
SC_S_3	2.08	2.08	2.08	2.41	2.41	2.41	2.04	2.04	2.04	-	-

(*) condition of eq. 7 satisfied by reducing the value of the degradation ultimate slip $v_{u,deg}$

(**) condition of eq. 7 not satisfied

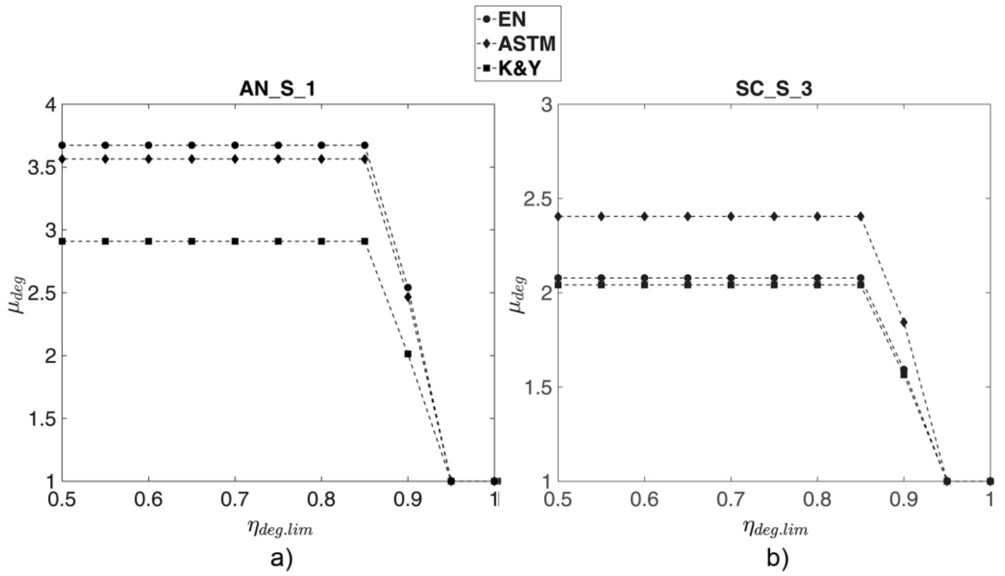

Figure 18: $\boldsymbol{\mu_{deg}}$ vs $\boldsymbol{\eta_{deg,lim}}$ curves for tests AN_S_1, and SC_S_3 ($\tilde{f}_{deg,lim} = \mathbf{0.8}$)

A negligible influence of the strength degradation in the calculation of μ_{deg} was observed for hold-downs, see Figure 19. However, differently from T2T and S2T connections, values of μ_{deg} lower than 2.70, 2.65 and 2.20 were calculated for EN12512 [9],] ASTM E2126 [2] and K&Y [28] procedures, respectively, as reported in Table 13. Since Hold-downs are not able to undergo medium-to-high amplitude plastic deformations, the degradation ultimate displacement $v_{u,deg}$ is triggered by the failure of the connection rather than the impairment of strength. For angle-brackets, values of ductility lower than 1.5 for all the three analysis methods were detected in case of $\eta_{deg,lim} = 0.8$; moreover, in two tests the condition of eq. 7 was not satisfied.

Table 13: Ductility μ_{deg} and $\tilde{f}_{deg}$ factor for mechanical anchors

Mechanical Anchors	μ_{deg}									$\tilde{f}_{deg}$	
	EN 12512			**ASTM E2126**			**K&Y**				
	w/o $\eta_{deg,lim}$	$\eta_{deg,lim}$ =0.7	$\eta_{deg,lim}$ =0.8	w/o $\eta_{deg,lim}$	$\eta_{deg,lim}$ =0.7	$\eta_{deg,lim}$ =0.8	w/o $\eta_{deg,lim}$	$\eta_{deg,lim}$ =0.7	$\eta_{deg,lim}$ =0.8	w/o $\eta_{deg,lim}$	$\eta_{deg,lim}$ =0.8
HD_SC_1	2.36	2.36	2.36	2.65	2.65	2.65	2.19	2.19	2.19	0.90	0.92
HD_AN_1	1.86	1.86	1.86	1.97	1.97	1.97	1.81	1.81	1.81	0.85	1.13
HD_AN_2	3.98	3.04	2.69	3.68	2.78	2.46	3.12	2.39	2.12	0.97	1.19
HD_AN_3	3.00	3.00	2.10	2.95	2.95	2.06	2.72	2.72	1.91	0.84	1.01
HD_AN_4	1.71	1.71	1.71	1.74	1.74	1.74	1.59	1.59	1.59	0.84	0.84
HD_AN_5	1.76	1.76	1.76	1.75	1.75	1.75	1.62	1.62	1.62	0.86	0.86
HD_AN_6	2.41	2.03	1.77	2.50	2.09	1.82	2.25	1.88	1.63	0.86	1.03
HD_AN_7	1.64	1.64	1.64	1.74	1.74	1.74	1.53	1.53	1.53	1.02	1.02
HD_AN_8	3.35	2.81	2.46	3.36	2.84	2.48	2.66	2.23	1.95	0.94	1.10
HD_OSB_1	3.72	3.72	3.72	3.78	3.78	3.78	3.09	3.09	3.09	0.85	1.09
HD_GFB_1	4.01	4.01	3.20	3.90	3.90	3.11	3.31	3.31	2.64	0.70	0.97
AB_1	1.13	1.13	1.13	1.39	1.39	1.39	1.29	1.29	1.29	1.22	1.22
AB_2	2.03	1.90	1.36**	2.17	2.03	1.45**	1.86	1.74	1.24**	0.90	0.73
AB_3	1.67	1.57	1.15**	1.79	1.69	1.23**	1.66	1.56*	1.14**	0.85	0.69

(*) condition of eq. 7 satisfied by reducing the value of the degradation ultimate slip $v_{u,deg}$

(**) condition of eq. 7 not satisfied

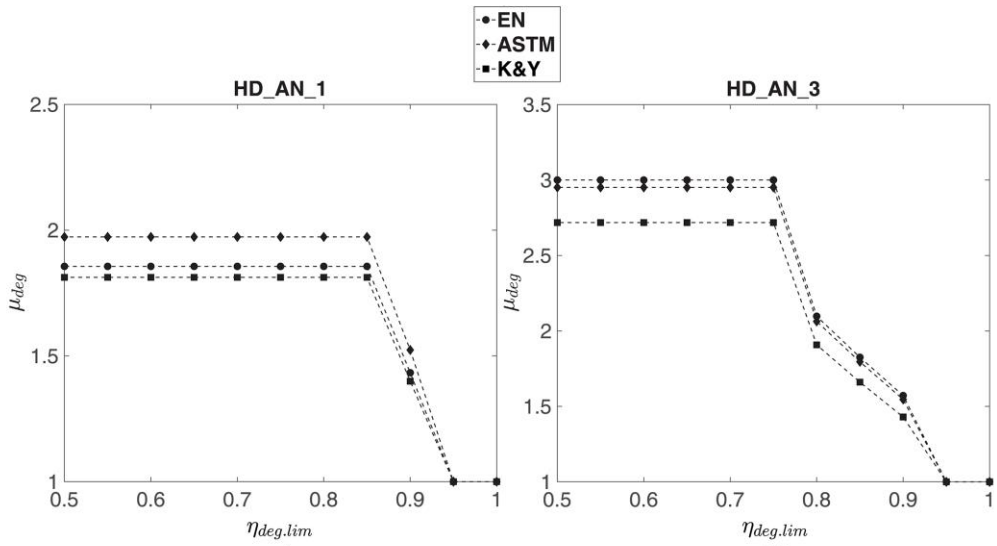

Figure 19: μ_{deg} vs $\eta_{deg,lim}$ curves for tests HD_AN_1 and HD_AN_3 ($\tilde{f}_{deg,lim} = 0.8$)

4.3 Discussion

In relation to the results reported in Sections 4.1 and 4.2, the following conclusions can be drawn.

- The impairment of strength factor η_{deg} vs dimensionless slip amplitude $\tilde{v}$ curves is an efficient tool to evaluate the low-cycle strength of dissipative connections, establishing a relationship between strength degradation and amplitude deformations. A negligible dependency of η_{deg} from $\tilde{v}$, analytically described by values of the coefficient a close to zero, $\eta_{deg,\tilde{v}=1}$ close to 1 and high values of $\tilde{v}_u$, characterizes connections with a good low-cycle fatigue strength such as dowelled connections or 10 mm screwed T2T connections. Connections with a poor low-cycle fatigue strength conversely show low values of η_{deg} and $\tilde{v}_u$.
- For a dimensionless slip amplitude close to 1, the impairment of strength $\eta_{deg,\tilde{v}=1}$ is not lower than 0.9 for most tested connections. As expected, significant values of the impairment of strength are obtained only for medium-to-high plastic deformations.
- The timber connections exhibited different levels of capacity in terms of ductility and strength degradation. Smooth nailed, 10 mm diameter screwed and dowelled connections are able, in most cases, to undergo medium-to-high-amplitude plastic deformations with a limited impairment of strength between the 1st and 3rd cycle. Some stapled connections and most of 8 mm screwed connections showed medium-to-high levels of ductility with a non-negligible impairment of strength whereas 6 mm screws and mechanical anchors were not able to undergo medium-to-high plastic deformations.
- In relation to the values of ductility capacity achieved for different limit values of the impairment of strength factor, four different categories for the tested connections are proposed, see Table 14. The first category (i) includes the connections able to achieve

values of μ_{deg} equal or higher than 6 for a value of $\eta_{deg,lim}$ equal to or higher than 0.8, $\mu_{deg}(\eta_{deg,lim}=0.8)\geq 6$. In the second category (ii) the connections are included able to achieve values of μ_{deg} equal or higher than 4 for a value of $\eta_{deg,lim}$ equal to or higher than 0.8, $\mu_{deg}(\eta_{deg,lim}=0.8)\geq 4$**.** The third category (iii) includes the connections with a ductility capacity μ_{deg} equal to or higher than 4, without taking into account any limit value of the impairment of strength factor, $\mu_{deg}(\mathrm{w}\ /\ o\ \eta_{deg,lim})\geq 4$**.** The connections not able to achieve a ductility capacity equal or higher than 4 for any value of the impairment of strength belong to the fourth category (iv).

Table 14: categories of connections in terms of ductility capacity and cycle fatigue strength, $\boldsymbol{\eta_{deg,lim}=0.8}$

Connections	*Category*			
	(i)	*(ii)*	*(iii)*	*(iv)*
	$\mu_{deg}(\eta_{deg,lim}=0.8)\geq 6$	$\mu_{deg}(\eta_{deg,lim}=0.8)\geq 4$	$\mu_{deg}(\mathrm{w}\ /\ o\ \eta_{deg,lim})\geq 4$	$\mu_{deg}(\mathrm{w}\ /\ o\ \eta_{deg,lim})<4$
P2T	SN_OSB_1,2,3;	RN_OSB_2,3,4 SN_GFB_1	ST_OSB_1,3 ST_GFB_1,3	ST_OSB_2 ST_GFB_2
T2T	SC_GLT_6 SC_CLT_3 D_CLT_3	SC_GLT_4,5 SC_CLT_2	SC_GLT_1,3 SC_CLT_1	SC_GLT_2
S2T	-	AN_S_2	-	AN_S_1,3 SC_S_1,2,3
MA	-	-	HD_GFB_1	HD_SC_1 HD_AN_1 to 8 HD_OSB-1 AB_1,2,3

If a value of $\eta_{deg,lim}$ equal to 0.7 was assumed, connections SC_GLT_4,5, SC_CLT_1 and SN_GFB_1 would move from category (ii) to category (i) in Table 14. On the contrary, RN_OSB_2,3,4 and AN_S_2 would still belong to category (ii) also in this case.

- The proposal of introducing the strength degradation as an additional condition for the evaluation of ultimate slip significantly reduces the values of ductility for connections which belong to categories ii) and iii). On the contrary, dowelled connections and 10 mm screwed connections in tests D_CLT_1, SC_GLT_6, SC_CLT_3 show quasi-constant value of ductility independently on strength degradation. A similar behaviour was observed for most of connections in category iv). In this case, however, the low influence of strength degradation is due to their low capacity to undergo medium-to-high plastic deformation; the connections fail for values of slip amplitude not far from yield slip without exhibiting, for this reason, a significant degradation.

- As highlighted by Munoz et al. [32], a significant difference in terms of values of ductility capacity is obtained by applying different methods for the evaluation of the yield slip in case of connections which exhibit a large post yielding behaviour. The values of ductility calculated according to EN12512 [9] are in most cases higher than the values obtained from K&Y [28] and ASTM E2126 [2].

5. Conclusions

In this paper, a new methodology to determine the low-cyclic fatigue strength of different typologies of dissipative timber connections is presented. 44 experimental tests with various configurations from four research projects were analysed and discussed in order to evaluate the strength degradation as an additional condition for the calculation of the ultimate slip in low-cyclic tests. A linear relationship between the impairment of strength and the slip amplitude was established for all tested connections. The ductility capacity was calculated according to the procedure of EN12512 [9], K&Y [28] and ASTM E2126 [2] for different limit values of the impairment strength factor. Four categories of connections in terms of ductility capacity and strength degradation were proposed. Timber-to-timber connections with smooth nails, 10 mm diameter screws and 12 mm dowels were able, in most cases, to achieve medium-to-high values of ductility without a significant strength degradation. Most of 8 mm screwed timber-to-timber connections and some of stapled panel-to-timber connections were able to undergo medium-to-high levels of ductility only accepting high values for the impairment of strength between the 1st and the 3rd cycle. 6 mm screwed timber-to-timber connections and mechanical anchors were not able to achieve high values of ductility independently on the limit values adopted for the strength degradations.

Acknowledgments

This study was partially funded by a FederLegno Arredo (Italy) grant. Some of the experimental tests were carried out within the X-Rev project, funded by the Province of Bolzano (Italy) and Rothoblaas Company, OptimberQuake project (Optimization of Timber Multi-storey Buildings against Earthquake impact) funded by the German Federal Ministry of Economy and Energy as part of the CORNET programme of the European Commission (Grant EN 50) and OptimberquakeCheck project (Development of a method for the reliable and simple evaluation of the earthquake resistance of single to four-story timber buildings and simple hall structures in zones of low and medium seismicity) funded by the German Federation of Industrial Research Associations (AiF, iVTH, IGF 19260N). Special thanks go to Marco Luchetti (FederLegno Arredo) for his support to this study.

References

1. American Forest & Paper Association- AFPA (2005) National Design Specification NDS for wood construction— commentary. (2005) ed. Washington (DC, USA): American Forest & Paper Association.

2. American Society Standard Method (ASTM) E2126 - 11(2018) - Standard Test Methods for Cyclic (Reversed) Load Test for Shear Resistance of Vertical Elements of the Lateral Force Resisting Systems for Buildings.

3. ANSI/AISC 341-10 (2010) Seismic Provisions for Structural Steel Buildings, American institute of steel construction.

4. Ceccotti A, Sandhaas C, Okabe M, Yasumura M, Minowa C, Kawai N (2013) SOFIE project - 3D shaking table test on a seven-storey full-scale cross-laminated building. Earthquake Engineering & Structural Dynamics, 42(13): 2003-2021, doi: 10.1002/eqe.2309.

5. Commonwealth Scientific and Industrial Research Organization (CSIRO). 1996. Timber evaluation of mechanical joint systems. Part 3, Earthquake loading. CSIRO, Melbourne, Australia

6. D’Arenzo G., Rinaldin G., Fossetti M., Fragiacomo M. (2019) An innovative angle shear-tension angle bracket for Cross-Laminated Timber structures: Experimental tests and numerical modelling. Eng Struct 2019;197: 109434. https://doi.org/10.1016/j.engstruct.2019.109434

7. Dean, J.A., (1988). “The Ductility of Nailed Sheathing Joints in Timber Framed Shearwalls.” Report CE 88/14, Civil Engineering Department, University of Canterbury, Christchurch, New Zealand.

8. Dolan, J.D. and Madsen, B., (1992). “monotonic and Cyclic Nail Connection Tests.” Canadian Journal of Civil Engineering 19:97-104.

9. EN 12512:2001/A1:2005, Timber structures – Test methods –cyclic testing of joints made with mechanical fasteners. Brussels, Belgium: CEN.

10. EN 26891:1991, Timber structures - Joints made with mechanical fasteners - General principles for the determination of strength and deformation characteristics. Brussels, Belgium: CEN, European Committee for Standardization.

11. EN 1998-1:2004+A1:2013, Eurocode 8 - Design of structures for earthquake resistance part 1: General rules, seismic actions and rules for buildings. Brussels, Belgium: CEN, European Committee for Standardization.

12. Filiatrault A, Christovasilis IP, Wanitkorkul A, Van de Lindt JW (2010) Experimental seismic response of a full-scale light-frame wood building. Journal of Structural Engineering, 136(3): 246-254, doi: 10.1061/(ASCE)ST.1943-541X.0000112.

13. Fischer, D. P. Filiatrault A., Folz B., Uang C., Seible F.(2001). Two-story single family house shake table test data. Richmond, Calif. : CUREE, 2001.

14. Flatscher G, Bratulic K, Schickhofer G. (2015) Experimental tests on cross-laminated timber joints and walls. Proc. ICE Struct Build 2015; 168(11):868–77. http://dx.doi.org/10. 1680/stbu.13.00085.

15. Foliente G.C. (1996) Issues in seismic performance testing and evaluation of timber structural systems. In: Proceedings of the 1996 international timber engineering conference. vol. 1. p. 1.29–.36.

16. Follesa M, Fragiacomo M, Casagrande D, Tomasi R, Piazza M, Vassallo D, Canetti D, Rossi S. (2018) The new provisions for the seismic design of timber buildings in Europe. Eng Struct 2018;168:736–47. http://dx.doi.org/10.1016/j.engstruct.2018.04.090.

17. Fonseca, F. S., Rose, S. K., Campbell, S. H. (2002) Nail, wood screw, and staple fastener connections. CUREE publication; W-16, Richmond, Calif. : CUREE, 2002.

18. Gavric I, Fragiacomo M, Ceccotti A. (2015a) Cyclic behaviour of typical metal connectors for cross-laminated (CLT) structures Eur J Wood Wood Prod 2015;73(2):179–91. http://dx.doi.org/10.1007/s00107-014-0877-6.

19. Gavric I., Fragiacomo M., Ceccotti A. (2015b) Cyclic behavior of typical screwed connections for cross-laminated (CLT) structures. Materials and Structures/Materiaux et Constructions 48(6), pp. 1841-1857

20. Germano, F., Metelli, G., Giuriani, E. (2015) Experimental results on the role of sheathing-to-frame and base connections of a European timber framed shear wall. Construction and Building Materials, 80, pp. 315-328, doi: 10.1016/j.conbuildmat.2015.01.076.

21. He M., Lam F., and Prion H.G.L.(1998) Influence of cyclic test protocols on performance of wood-based shear walls in Can. J. Civ. Eng. 25: 539–550.

22. Hossain A, Danzig I, Tannert T. (2016) Cross-laminated timber shear connections with double-angled self-tapping screw assemblies. J Struct Eng 2016;142(11):04016099. http://dx.doi.org/10.1061/(ASCE)ST.1943-541X.0001572.

23. ISO 16670:2003. Timber structures -- Joints made with mechanical fasteners - Quasi-static reversed-cyclic test method.

24. Izzi M., Casagrande D., Bezzi S., Pasca D., Follesa M., Tomasi R., (2018) Seismic behavior of cross-laminated timber structures: A state-of-the-art review", Engineering Structures, 170 (2018), 42–52. doi: 10.1016/j.engstruct.2018.05.060.

25. Izzi M., Polastri A. (2019) Low cycle ductile performance of screws used in timber structures, Construction and Building Materials 217, pp. 416-426.

26. Jorissen A., Fragiacomo, M. (2011) General notes on ductility in timber structures. Engineering Structures, 33 (11), 2011, pp. 2987-2997.

27. Karacabeyli E, Ceccotti A. (1998) Nailed wood-frame shear walls for seismic loads: Test results and design considerations. Struct Eng World Wide 1998; Paper ref. T207-6.

28. Kobayashi, K., and Yasumura, M. (2011). Evaluation of plywood sheathed shear walls with screwed joints tested according to ISO 21581. CIB-W18 Paper 44–15, Alghero, Italy.

29. Krawinkler, H.; Parisi, F.; Ibarra L.; Ayoub A.; Medina R. (2001): Development of a Testing Protocol for Woodframe Structures. CUREE Publication No. W-02, 2001.

30. Liu J., Lam F. (2018) Experimental test of coupling effect on CLT angle bracket connections, Eng Struct, 171C (2018), pp. 862-873.

31. Liu J., Lam F. (2019) Experimental test of coupling effect on CLT hold-down connections, Eng Struct, Engineering Structures, Volume 178, 1 January 2019, pp. 586-602.

32. Mahaney J. A., Kehoe B.E. (2002) Anchorage of Woodframe Buildings : Laboratory Testing Report. Richmond, Calif. CUREE, 2002.

33. Muñoz W, Mohammad M, Salenikovich A, Quenneville P. (2008) Need for a harmonized approach for calculations of ductility of timber assemblies. In: Proceedings of the meeting 41 of the working commission W18-timber structures. CIB 2008.

34. Pei S, van de Kuilen J-WG, Popovski M, Berman JW, Dolan JD, Ricles J, et al. (2016) Cross-Laminated Timber for seismic regions: progress and challenges for research and implementation. J Struct Eng 2016;142(4):E2514001. http://dx.doi.org/10.1061/(ASCE)ST.1943-541X.0001192.

35. Peterson,J.(1983). Bibliography on lumber and wood panel diaphragms. J. Struct. Eng., 10.1061/(ASCE)0733-9445(1983)109:12(2838), 2838–2852.

36. Piazza, M., Polastri, A., Tomasi, R. (2011) Ductility of timber joints under static and cyclic loads Proceedings of the Institution of Civil Engineers: Structures and Buildings, 164 (2), pp. 79-90. doi: 10.1680/stbu.10.00017.

37. Popovski M, Gavric I (2016) Performance of a 2-story CLT house subjected to lateral loads. Journal of Structural Engineering, 142(4): E4015006(1-12), doi: 10.1061/(ASCE)ST.1943-541X.0001315.

38. Pozza L., Ferracuti B., Massari M., Savoia M. (2018) Axial-Shear interaction on CLT hold-down connections–Experimental investigation, Eng Struct, 160 (2018), pp. 95-110.

39. Rinaldin G, Fragiacomo M. (2016) Non-linear simulation of shaking-table tests on 3- and 7storey X-Lam timber buildings. Eng Struct 2016;113:133–48. http://dx.doi.org/10.1016/j.engstruct.2016.01.055.

40. Sartori, T., Tomasi, R. (2013) Experimental investigation on sheathing-to-framing connections in wood shear walls in Engineering Structures, 56, pp. 2197-2205. doi: 10.1016/j.engstruct.2013.08.039.

41. Schneider J, Karacabeyli E, Popovski M, Stiemer SF, Tesfamariam S. (2014) Damage assessment of connections used in Cross-Laminated Timber subject to cyclic loads. J Perform Constr Facil 2014;28(6):A4014008. http://dx.doi.org/10.1061/(ASCE)CF. 1943-5509.0000528.

42. Seim W., Kramar M., Pazlar T., Vogt T. (2015) OSB and GFB as sheathing materials for timber-framed shear walls: Comparative study of seismic resistance. Journal of Structural Engineering, Volume 142, Issue 4. doi: 10.1061/(ASCE)ST.1943-541X.0001293.

43. Stewart, W.G.,(1987). The Seismic Design of Plywood Sheathed Shearwalls, thesis submitted in partial fulfillment of the Doctor of Philosophy Degree at the University of Canterbury, New Zealand.

44. Casagrande D., Grossi P., Tomasi R. (2016) Shake table tests on a full-scale timber-frame building with gypsum fibre boards. European Journal of Wood and Wood Products, 74(3): 425-442, doi: 10.1007/s00107-016-1013-6

45. Tomasi R, Smith I. (2015) Experimental characterization of monotonic and cyclic

loading responses of CLT panel-to-foundation angle bracket connections. J Mater Civ Eng 2015;27(6):04014189. http://dx.doi.org/10.1061/(ASCE)MT.1943-5533.0001144.

46. Van de Lindt, J. W. (2004). Evolution of wood shear wall testing, modeling, and reliability analysis: Bibliography Pract. Period. Struct. Des. Constr., Vol. 9, Issue 1, https://doi.org/10.1061/(ASCE)1084-0680(2004)9:1(44) .

47. Van de Lindt JW, Pei S, Pryor SE, Shimizu H, Isoda H (2010) Experimental seismic response of a full-scale six-story light-frame wood building. Journal of Structural Engineering, 136(10): 1262-1272, doi: 10.1061/(ASCE)ST.1943-541X.0000222.

48. Yasumura, M.,Kawai, N. (1998). Estimating seismic performance of wood-framed structures. Proc., 5th World Conf. on Timber Engineering (WCTE), Montreaux, Switzerland, Vol. 2, 564–571

49. Yasumura M, Kobayashi K, Okabe M, Miyake T, Matsumoto K (2016) Full-scale tests and numerical analysis of low-rise CLT structures under lateral loading. Journal of Structural Engineering, 142(4): E4015007(1-12), doi: 10.1061/(ASCE)ST.1943541X.0001348

50. prEN 14592 (2017). Timber structures — Dowel-type fasteners — Requirements; CEN/TC 124